Mémoire de stage

présenté par
Sylvain SCHMITT

pour obtenir le diplôme national de master
mention Biodiversité, écologie, évolution
parcours Biodiversité végétale et gestion des écosystèmes tropicaux (BIOGET)

Sujet :
A COMPLETER

soutenu publiquement le XX.xxxx.201X
à Kourou

devant le jury suivant :

Dr Bruno HÉRAULT *Tuteur de stage*
Titre Prénom NOM *Examinateur*
Titre Prénom NOM *Examinateur*
Dr Stéphane TRAISSAC *Enseignant-réferent*

Les opinions émises par les auteurs sont personnelles et n'engagent pas AgroParisTech.

Contents

Résumé et Abstract

Écrire le résumé français ici...

Write the english abstract here...

Acknowledgments

I would like to thank...

- Bruno
- Stéphane
- Laurent
- Fabian
- Isabelle
- Jérôme
- Camilla
- Aurélie
- Éric
- ...

Introduction

Sutainable forest management in the tropics (i.e. managed selective harvesting of timber) has been widely promoted internationnaly to combat tropical deforestation and degradation [Zimmerman and Kormos, 2012]. Currently tropical logging accounts for one eight of global timber production [Blaser et al., 2011] and is still increasing. Most tropical timber production originates from selective logging, the targeted harvesting of timber from commercial species in a single cuttint cycle [Martin et al., 2015].

On the other hand, tropical rainforests have fascinated ecologists due to their outstanding diversity [Connell, 1978]. Effectively tropical forests host over half of the Earth's biodiversity [Scheffers et al., 2012]. High biodiversity from tropical rainforests is the source of many ecosystem functions. Amongst others, tropical forests play a key role in biogeochemical cycles, including carbone storage [Lewis et al., 2004]. **Add insights into carbon storage role of tropical forest.** Ecosystem functions from tropical forests support numerous ecosystem services, such as timber production and climate regulation.

But several authors argue that selective logging represents a major threat to biodiversity [Carreño-Rocabado et al., 2012, de Avila et al., 2015, Gibson et al., 2013, Martin et al., 2015, Zimmerman and Kormos, 2012], challenging the sustainable definition from current selective logging. We consequently need to assess both short and long term impacts of selective logging on tropical forest ecosystems to implement better syslvicultural practives in order to reach sustainability.

The question of selective logging impact on tropical forest can be directly related to the emerging field of biodiversity and ecosystem functionning [Loreau, 2000]. Tropical forest outstanding biodiversity will be both a factor and a result of forest ecosystem response to logging disturbance. And forest ecosystem response to logging disturbance will directly modify ecosystem functionning in both short and long term. Consequently assessing selective logging effect on tropical forest linking biodiversity and ecosystem seems an obvious and promising way [Loreau, 2010]. **Paragraph to fully review !**

Negative short term impacts of selective logging have been assessed [Carreño-Rocabado et al., 2012; de Avila et al., 2015; but see Martin et al., 2015]. Much less is known about the long term impact [Osazuwa-Peters et al., 2015]. The main reason is the difficulty to conduct long term empirical study [but see Herault et al., 2010], which can be completed by the use of forest simulators [Huth et al., 2004, Köhler and Huth, 2004, Rüger et al., 2008, Tietjen and Huth, 2006]. Individual-based models of forest dynamics present the perfect framework to develop such joint biodiversity-ecosystem approaches [Maréchaux and Chave]. Individual-based models describe forest 'patches' accumulating carbon through time, assessing tree growth within the patch, or releasing carbon through gap opening [Bugmann, 2001]. Up to several dozens of different Plant Functional Types (PFTs) are generally defined and models can sometimes be fully spatially explicit [Pacala et al., 1996]. Recently, the forest growth simulator TROLL [Chave, 1999], an individual-based and spatially explicit forest model, was developped to introduce recent advances in plant physiological community. TROLL model relates physiological processes to species-specific functional traits [Maréchaux and

Chave]. Consequently, TROLL model allow to simulate fully a neotropical forest biodiversity to study biodiversity-ecosystem functionning link response to logging disturbance.

Major question greater diversity (taxonomic and functional) brought a better resilience to disturbance ?

Model description

Overview

TROLL model each tree indivdually in a located environment. Thus TROLL model, alongside with SORTIE [Pacala et al., 1996, Uriarte et al., 2009] and FORMIND [Fischer et al., 2016, Köhler and Huth, 1998], can be defined as an individual-based and spatially explicit forest growth model. TROLL simulates the life cycle of individual trees from recruitment, with a diameter at breast height (dbh) above 1 cm, to death with growth and seed production. Trees are growing in a located light environment explicitly computed witin voxels of 1 m^3. Each tree is consistently defined by its age, diameter at brest height (dbh), height (h), crown radius (CR), crown depth (CD) and leaf area (LA) (see figure 1). Tree geometry is calculated with allometric equations but leaf area vary dinamically within each crown following carbon allocations. Voxels resolution of 1 m^3 allow the establishment of maximum one tree by 1x1 m pixels. Each tree is flagged with a species label inherited from the parent tree through the seedling recruitment. A species label is associated to a number of species specific parameters (see table 1) related to functional trait values which can be sampled on the field.

Carbon assimilation is computed over half-hourly period of a representative day. Then allocation is computed to simulate tree growth from an explicit carbone balance (in contrast to previous models). Finally environment is updated at each timestep set to one month. Seedlings are not simulated explicitly but as a pool. In addition belowground processes, herbaceous plants, epiphytes and lianas are not simulated inside TROLL. The source code is written in C++ and available upon request. All modules of TROLL models are further detailed in Appendix 1: TROLL model.

Table 1: Species-specific parameters used in TROLL from Maréchaux and Chave. Data originates from the BRIDGE [Baraloto et al., 2010] and TRY [Kattge et al., 2011] datasets.

Abbreviation	Description	Units
LMA	leaf mass per area	$g.m^{-2}$
N_m	leaf nitrogen content per dry mass	$mg.g^{-1}$
P_m	leaf phosphorous content per dry mass	$mg.g^{-1}$
wsg	wood specific gravity	$g.cm^{-3}$
dbh_{thresh}	diameter at breasth height threshold	m
h_{lim}	asymptotic height	m
a_h	parameter of the tree-height-dbh allometry	m

Previous implementation of TROLL model used Reich et al. [1991] allometry to infer leaf lifespan LL from species leaf mass per area LMA [Maréchaux and Chave, see Appendix 1: TROLL model].

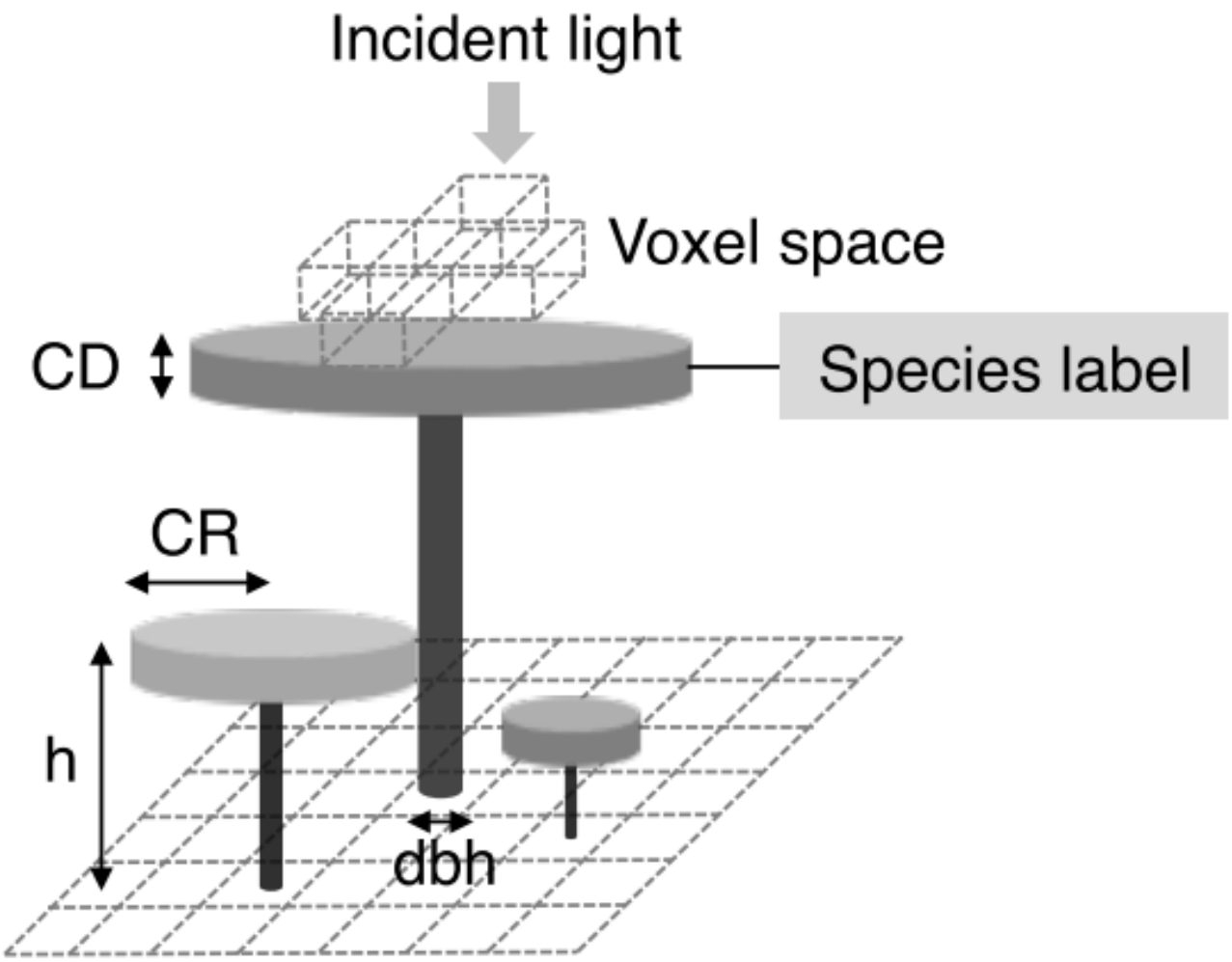

Figure 1: Individuals tree inside TROLL explicit spatial grid from Maréchaux and Chave. Tree geometry (crown radius CR, crown depth CD, height h, diameter at breast height dbh) is updated at each timestep following allometric relationship with assimilated carbon allocated to growth. Each tree is flagged with a species label linking to its species-specific attributes. Light is compputed explicitly at each timestep for each voxel.

But the use of the allometrie from Reich et al. [1991] with current implementation of the TROLL model resulted in an underestimation of leaf lifespan for low LMA species. Consequently in the following paragraph we suggest a new allometry.

Selective logging is defined as the targeted harvesting of timber from species of interest. Consequently, tropical sylviculture can be assimilated to a disturbance. The main difference between a disturbance and selective logging is the targetting of both species and individuals of interest. So we decided to first asses unselective disturbance effect on tropical forest ecosystem to subsequently better understand selective logging effect. First, we implemented a disturbance module inside TROLL model to simulate unselective disturbance. Secondly, we implemented a sylviculture module inside TROLL model to simulate selective logging in regards to french Guiana practices.

Leaf lifespan

The underestimation of leaf lifespan for low LMA species with the allometry from Reich et al. [1991] resulted in indivduals unealistic early death from carbon starvation. We gathered data from TRY[Kattge et al., 2011], DRYAD [Chave et al., 2009] and GLOPNET [Wright et al., 2004] datasets. We used an out of the bag method applied on a random forest to select variables with highest importance to explain leaf lifespan. We thus selected leaf mass per are LMA, leaf nitrogen content N and wood specific gravity wsg. We then used a bayesian approach to test different models with growing level of complexity. The model with the best tradeoff between complexity (number of parameters), convergence, likelihood, and prediction quality (root mean square error of prediction RMSEP) was kept. We selected following model with a maximum likelihood of 13.6 and a RMSEP of 12 months:

$$LL_d \sim log\mathcal{N}(\beta_{1_d} * LMA - \beta_{2_d} * N * \beta_3 * wsg, \sigma) \tag{1}$$

Leaf lifespan LL follows a lognormal law with location infered from leaf lifespan LMA, nitrogen content N and wood specific gravity wsg and a scale σ. Each β_{i_d} is following a normal law located on β_i with a scale of σ_i. All β_i, σ_i, and σ are assumed without presemption following a gamma law. d represents the dataset random effects and encompass environmental and protocol variations (see Appendix 2: Leaf lifespan model for more details).

Disturbance

Disturbance module was designed in the simplest way in order to relate the ecosystem answer to volume lost without any individuals nor species targetting. For a given iteration $disturb_{iter}$, individuals are picked randomly with a uniform law on the number of trees. Selected individuals are then removed without trigerring a treefall to avoid any side effect. The operation is repeated untill the disturbance result in a defined lost basal area ($disturb_{intensity}$ in % of BA).

Sylviculture

In french guiana context sylviculture can be narrow to selective logging, which can be split in two steps: selection and harvesting. Selection encompass choice of the havrestable area, tree designation by the forest office, tree selection by the harvester, and removal off tree probbed as rotten by the lumber. Harvesting encompass tree felling, tracks opening, and long term damages (simplified in gap damages in current TROLL implementation).

Designation and selection

One major limit of current implementation of TROLL model is that it assumes a flat environment. Consequently the whole simulated area inside TROLL is considered has an harvestable zone. With all commercial species minimum and maximum harvestable diameter, TROLL calculates the total harvestable volume V_{htot}. If the total harvestable volume V_{htot} exceed 30 $m^3.hectare^{-1}$, commercial species minimum harvestable diameter dbh_{min} is increased untill V_{htot} is inferior to that upper limit.

In french guiana, tree harvesters are focusing on few species with easier marketable wood, resulting in a tree harvest around 20 $m^3.ha^{-1}$ (Laurent Descroix, ONF, personnal communication). TROLL ranks each commercial species on its economic value, and randomly remove individuals from lowest rank species untill it reaches total harvested volume V_{hdtot} (V_{hdtot} was set to 25 $m^3.hectare^{-1}$ in subsequent simulations).

Rotten trees

20 to 30 % of designated trees are considered as rotten once probed by the lumberman, and thus not harvested. Rotten trees are not random and depends both on tree species and diameter. We gathered data from the forest office (ONF, Laurent Descroix, personnal communication) inventories precising if tree were probbed as rotten and their corresponding species and diameter. In addition, tree plots and sawed volume was informed. We then used a bayesian approach to model the link between tree species and diameter and their risk to be probbed as rotten by the lumberman. We test different models with growing level of complexity and kept the model with the best tradeoff between complexity (number of parameters), convergence, likelihood, and prediction quality (root mean square error of prediction RMSEP):

$$\begin{aligned} probbed\ rotten &\sim \mathcal{B}(P(probbed\ rotten)) \\ P(probbed\ rotten) &= logit^{-1}(\beta_0 + \beta_1 * dbh) = \frac{e^{\beta_0+\beta_1*dbh}}{1+e^{\beta_0+\beta_1*dbh}} \end{aligned} \tag{2}$$

Tree *probbed rotten* follows a *Bernoulli* law of probability $P(probbed\ rotten)$. The odds for a tree to be probbed as rotten are calculated with the sum of a base odd to be rotten β_0 and a diameter dependent odd calculated with β_1. The probability for a tree to be probbed as rotten

$P(probbed\ rotten)$ is finally calculated by taking the inverse logit $logit^{-1}$ of the odd (see Appendix 3: Rotten tree model for more details).

Harvesting

Due to crown aspects, treefall from logs are often random (whereas difficult to manage, treefall can still be oriented, Laurent Descroix, ONF, personnal communication). Consequently, TROLL consider treefall from log as random like current natural treefall implementation inside TROLL (see code [Appendix 1]).

Tree harvesting roads are split in three classes: truck roads, main tractor track, and secondary track. Because TROLL assumes a flat environment, the main track is opened starting from the middle of one side of the simulated forest and untill it reaches the center with a width of 6 meters. In most cases, secondary tracks are opened once trees have been designated and the geolocation taken at a maximum distance of 30 meters from designated trees (Laurent Descroix, ONF, personnal communication). To simulate secondary tracks, TROLL uses a loads map, measuring every trees at a distance of 30 meters for each pixel, and a track proximity maps of the closest existing track. Next, the model select the pixel with the highest load and closest track, find the closest existing track and join it by removing tree in the way with a width of 5 meters. The operations are repeated untill no felt trees are left.

Gap damages

Most of models account long term damages due to selective logging with a 10 years increased mortality [Huth et al., 2004, Köhler and Huth, 2004, Rüger et al., 2008]. We decided to model explicitly long term logging damages because of their localised nature through a gap damages model. We gathered data from Paracou dataset [Guehl et al., 2004] in censuses between 1988 and 1992 on Paracou harvested plots. Individuals were categorized between alive, dead, or recruited during the period. We measured each individual distance to the closest gap. We then used a bayesian approach to test the link between tree death in the four years following the log event and distance to the closest gap. We adapted the model from Herault et al. [2010] based on a disturbance index into:

$$\begin{gathered} Death \sim \mathcal{B}(P(Death)) \\ P(Death) = logit^{-1}(\theta + \beta * e^{\alpha * d_{gaps}}) = \frac{e^{\theta+\beta*e^{\alpha*d_{gaps}}}}{1+e^{\theta+\beta*e^{\alpha*d_{gaps}}}} \end{gathered} \tag{3}$$

$Death$ of a tree follows a $\mathcal{B}⌉\nabla\backslash ı⊓↕↕⟩$ law of probability $P(Death)$. The odds for a tree to die are calculated with the sum of the natural tree death odd θ and a perturbation index $\beta * e^{\alpha * d_{gaps}}$. The perturbation index depend on the distance d_{gaps} of the tree i to the closest logging gap. The probability for a tree to die $P(Death)$ is finally calculated by taking the inverse logit $logit^{-1}$ of the odd.

Material and Methods

Sensitivity analysis

Maréchaux and Chave already assessed TROLL model sensitivity to several parameters (k see (9), ϕ see (32), $g1$ see (13), f_{wood} see (21), f_{canopy} see (23) and m see (28)) which they assumed having a key role in model functioning. On the other hand, we decided to use TROLL to study resistance and resilience of ecosystem face to disturbance, highlighting the role of biodiversity. Consequently we particulrarly needed to assess the importance of functional traits to further better control and evaluate functional diversities. We also needed to assess the sensitivity of TROLL model to the seed rain constant (n_{ext}, see (31)) because we assumed it as one of the main factors of tree recruitments after disturbance within simulations.

TROLL model currenty uses leaf mass per area (LMA in $g.m^{-2}$), leaf nitrogen content per dry mass (N_m in $mg.g^{-1}$), leaf phosphorus content per dry mass (P_m in $mg.g^{-1}$), wood specific gravity (wsg in $g.cm^{-3}$), diameter at breasth height threshold (dbh_{thresh} in m), asymptotic height (h_{lim} in m), and parameter of the tree-height-dbh allometry (a_h in m). To assess the sensitivity of TROLL model to species functionnal traits, we performed a sensitivity analysis by fixing species trait values to their mean. Each trait was tested independently. We reduce to a common mean traits with a Pearson's correlation value $r \geq 0.8$ (h_{max} and a_h with a correlation of $r = 0.98$). To assess the sensitivity of TROLL model to seed rain, we performed a sensitivity analysis by fixing simulations seed rain constant to 2, 20, 200 and 2000 seeds per hectare.

Simulations were conducted on Intel Xeon(R) with 32 CPUs of 2.00GHz and 188.9 GB of memory. We assumed maturity of the forest after 500 years of regeneration (Maréchaux & Chave) and computed simulation 100 years after a disturbance event with 40% loss of basal area. Due to computer limitations we did not run replicate (besides it should be necessary to reduce simulation stochasticity). To assess ecosystem outputs sensitivity to studied parameters, we compared it to 100 replicates of control simulations with all parameters set to default values. Ecosystem outputs outside of the range of the control replicates values are significantly influenced by the studied parameter.

Design of experiment

In order to assess the role of biodiversity in ecosystem answer to both disturbance and sylviculture, we needed to create a space of experiments encompassing both variation of disturbance, biodiversity and time. Disturbance was represented by percentage of basal area loss (0%, 25%, 50% and 75%), or as a selective logging simulation. Biodiversity was integrated with two components of its components: taxonomic and functional diversities. We used species richness SR to represents taxonomic diversity (5, 25, and 125 species). Functional diversity can be related to numerous

components, and Perrone et al. [2017] argued for 5: richness, divergence, regularity, overlap and mean. Because mature forest were created from a bare soil with TROLL simulations, we could not control a priori divergence, regularity and overlap but only assess theim before diturbance. Consequently, we focused on functional richness with convex hull volume CHV and functional mean with community weighted mean CWM. For each level of species richness SR, we selected 20 communities with growing convex hull volume CHV but with a community weighted means close to the regional species pool community weighted means. Effectivelly, we did not wanted drastic change in community means that could have more effect than functional richness itself. This design of experiments resulted in 60 communities (5 $SR * 20$ CHV) and 240 simulations (60 $communities * 4$ $levels\ of\ disturbance$) over 600 years (maturity being assumed after 500 years of regeneration [Maréchaux and Chave]). Figure 2 presents the design of experiment for communities biodiversity after the mature forest were simulated, and thus before disturbance. We obtained a broad range of both functionl dispersion $FDis$ and aboveground biomass AGB for simulated forest ecosystems before disturbance.

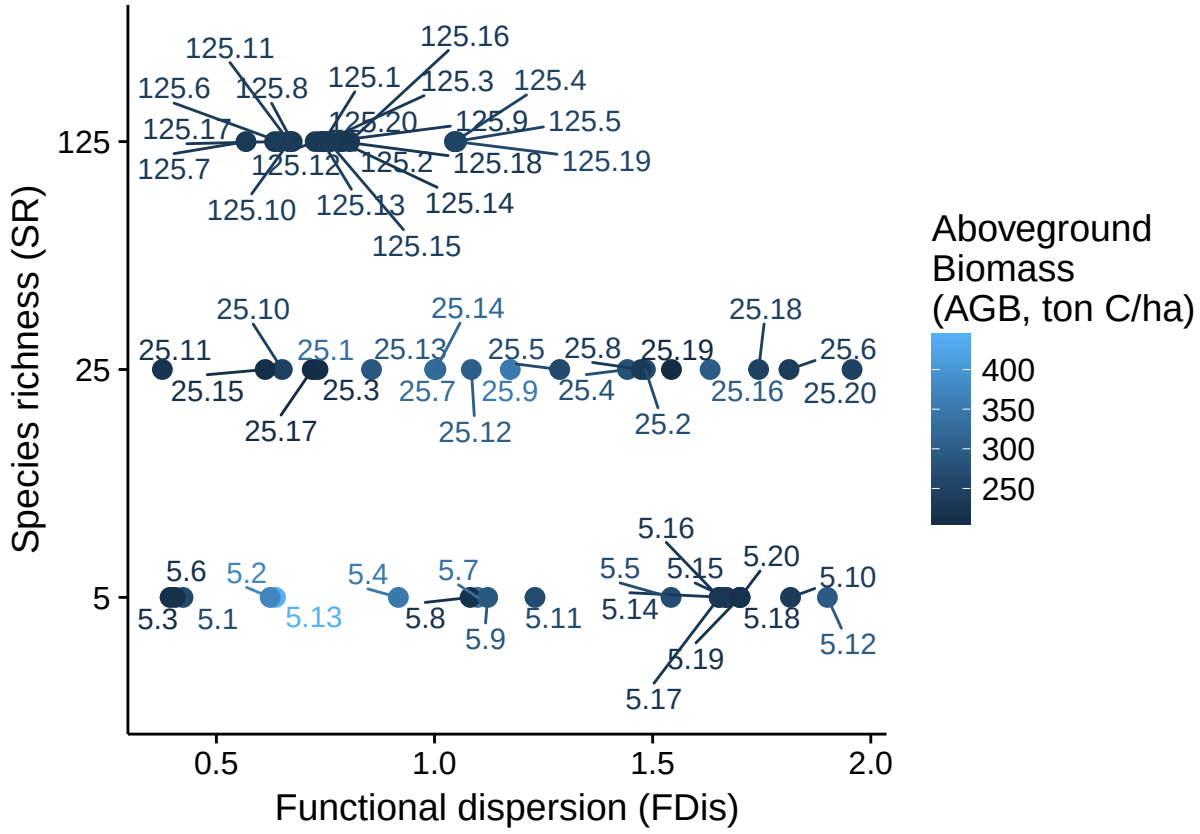

Figure 2: Experimental design before disturbance. Communities are implemented along a gradient of species richness (SR) and functional dispersion (FDis) resulting in a broad range of aboveground biomass (AGB). FDis was caluclated based on 4 functional traits (leaf mass per area, wood specific gravity, maximum diameter, and maximum height).

Ecosystem answer analysis

Ecosystem functions

Tropical forest ecosystems provides numerous ecosystem services linked to several ecosystem functions. We decided to describe simiulated tropical forests in two major functions: forest dynamic and forest production. Forest dynamic was represented by aboveground biomass (AGB in $ton\ C.ha^{-1}$), basal area (BA in $m^2.ha^{-1}$), total number of stem (N), number of stem above 10 cm diameter ($N10$), and number of stem above 30 cm diameter ($N30$). Forest production was represented by growth pimary productivity (GPP in $MgC.ha^{-1}$), net pimary productivity (NPP in $MgC.ha^{-1}$), tree autotrophic respiration in day ($Rday$ in $MgC.ha^{-1}$) and tree autotrophic respiration in night ($Rnight$ in $MgC.ha^{-1}$).

The resilience of metrics values post disturbance were assessed through Henry and Emmanuel Ramirez-Marquez [2012] formula:

$$R\left(t\right) = \frac{Recovery\left(t\right)}{Loss\left(t_d\right)} \approx \frac{X_T(t)}{X_C(t)} \tag{4}$$

The resilience of the system $R(t)$ at the time t is described by the ratio of recovery $Recovery(t)$ at time t to loss suffered $Loss(t_d)$ at disturbance time t_d. But in our peculiar case of tropical forest ecosystems, the equilibrium used to calculate $Loss(t_d)$ can not be reduced to a specific time if the equilibrium is dynamic. Consequently, to encompass undisturbed ecosystem variations throught time, we simulated an undisturbed control ecosystem C. And the resilience of the system $R(t)$ at the time t was defined as the ratio of the ecosystem metric values in the disturbed simulation $X_T(t)$ over the the ecosystem metric values from the control $X_C(t)$. Thus, the value of resilience $R(t)$ is normalized for all simulations and metrics. $R(t)$ will be equal to $R_{eq} = 1$ when reaching the equilibrium value. Consequently we can calculate an euclidean distance to equilibrium $d_{eq}(t)$ as $d_{eq}(t) = \sqrt{(R_{eq} - R(t))^2}$. Ecosystem euclidean distance to equilibrium was calculated in a multi-dimensional space for the two functions described above: forest dynamic (AGB, BA, N, N10, and N30) and forest production (GPP, NPP, Rday, and Rnight). We then used cummulative integral over time of eulcidean distance to equilibrium to assess simulations resilience.

Biodiversity effect

Biodiversity is not only a facet of the experimental design and an ecosystem output through forest diversity, but also interact on ecosystem functioning and consequently on its answer to disturbance. Biodiversity ecosystem functioning relation can be split in complementarity and selection effect with Loreau and Hector [2001] partitioning:

$$
\begin{aligned}
NE &= X_O - X_E = CE + SE \\
CE &= N * \overline{\Delta RX}\,\overline{M} \\
SE &= N * cov(\Delta RX, M)
\end{aligned}
\tag{5}
$$

Biodiversity net effect NE is based on the difference between ecosystem variable X observed value X_O within the community mixture of species and its expected value X_E if species performance were equal to their performance in monocultures. This effect can be partitioned between complementarity effect CE, representing niche partitionning, positive interactions, and resource supply, and selectvie effect SE due to dominant species pool driving the ecosystem. Both metrics depend on the variation of relative ecosystem variable ΔRX:

$$
\Delta RX_{sp} = \frac{X_{sp}(mixture)}{X_{sp}(monoculture)} - P_{sp} \tag{6}
$$

X_{sp} is the ecosystem variable value for one species either in mixture $X_{sp}(mixture)$ or in monoculture $X_{sp}(monoculture)$. P_{sp} is the proportion of the species in the mixture represented by species relative abundance. Consequently, CE averages diversity effects of all species presents in the mixture (both negatives and positives). Whereas SE become positive when dominant species outperform theimselves in mixture than in monoculture, and negative when less dominant species outperform theimselves in mixture than in monoculture [Tobner et al., 2016]. But similarly to resilience measurement, biodiversity net effect NE can be in a dynamic equilibrium and vary over time without disturbance. So in order to correctly assess selection and complementarity effect in answer to disturbance, we normalized it by undisturbed control ecosystem net effect NE_C to measure treatments net effect resilience $R(NE_T)$:

$$
R(NE_T) = \frac{NE_T}{NE_C} = \frac{SE_T}{NE_C} + \frac{CE_T}{NE_C} \tag{7}
$$

Resilience trajectories of ecosystem variable after disturbance were partitioned between complementarity effect CE and selection effect SE. In order to do that, the design of experiment was repeated for each species indivdually representing 652 simulations of monoculture.

Results

Sensitivity

Disturbance

Ecosystem functions

We transformed all ecosystem outputs from the 240 disturbance simulations in resilience metrics normalizing the treatment values by their corresponding control (Figure 3 A et B). We then gathered ecosystem outputs by main ecosystem functions (forest dynamic, forest production and forest diversity) to compute ecosystem distance to equilibrium (Figure 3 C). Finally, we integrated distance to equilibrium in a cummulative sum over time (Figure 3 D).

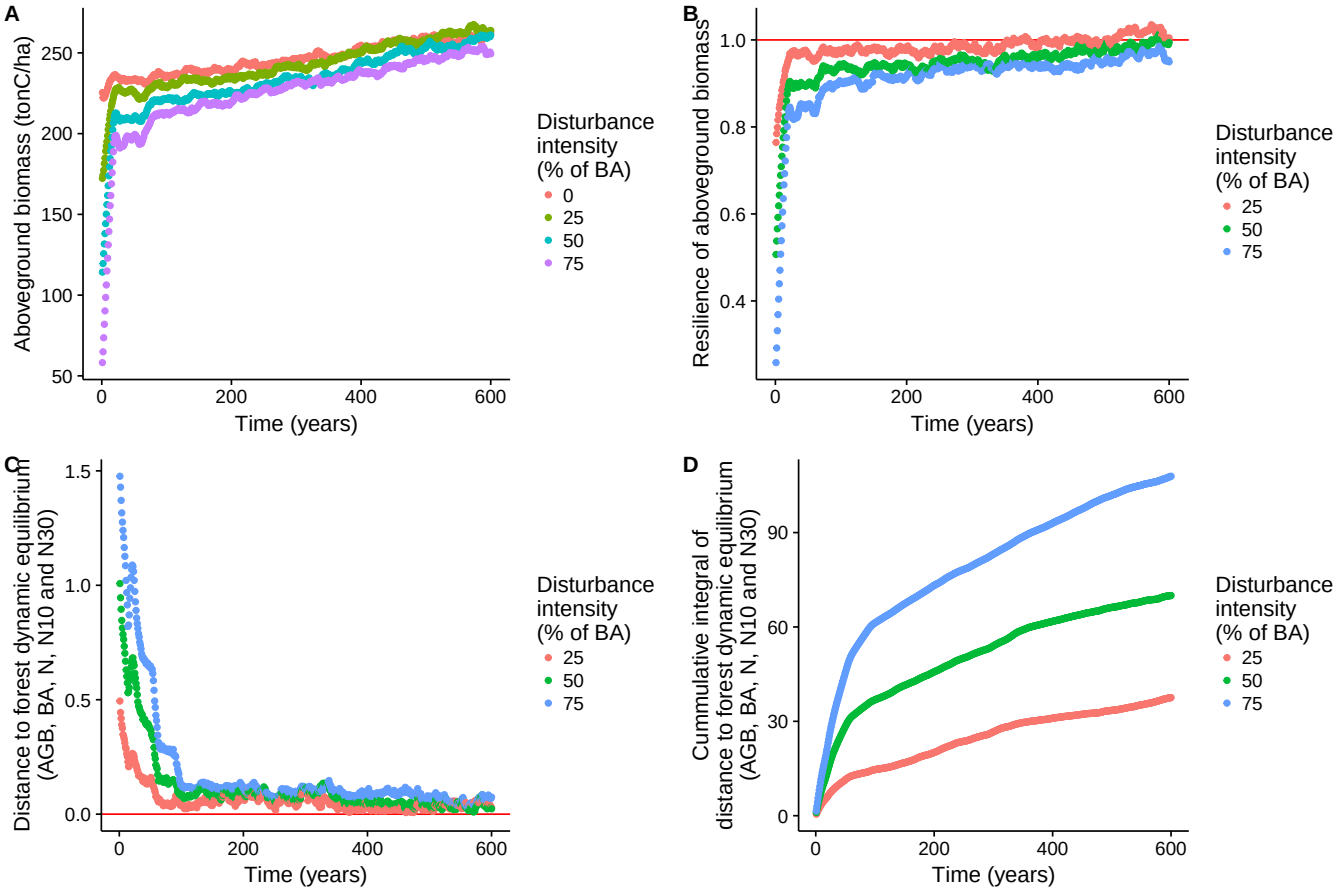

Figure 3: Ecosystem outputs data transformation. Ecosystem outputs (**A**) are normalized by the control value over time to calculate resilience (**B**); resilience of different ecosystem outputs is then used in a multidimensional space to caluclate ecosystem distance to equilibrium (**C**); finally distance ot equilibirum is integrated over time in a cummulative sum (**D**).

The ranking was stable over time for the 240 simulations. So we used the cummulative integral after 600 years Ieq_{600} as a measurement of ecosystem resilience. We compared cummulative integral after 600 years to communities taxonomic and functional diversity for each leavel of disturbance (see Figure 4). We found that increased functional diversity [FDiv, Villéger et al., 2008] was reducing cummulative integral from ecosystem distance to forest dynamic equilibrium after 600 years (Ieq_{600}). In addition, functional eveness was complementary reducing Ieq_{600}. Finally species richness was not directly link to Ieq_{600}. Effectivelly, low species richness could result in variant Ieq_{600}, but increased species richness resulted in increased functional diversity and consequently lower Ieq_{600}. We found similar results for all disturbance levels and other ecosystem functions (forest production and forest diversity, see Appendix 5: Disturbance simulations).

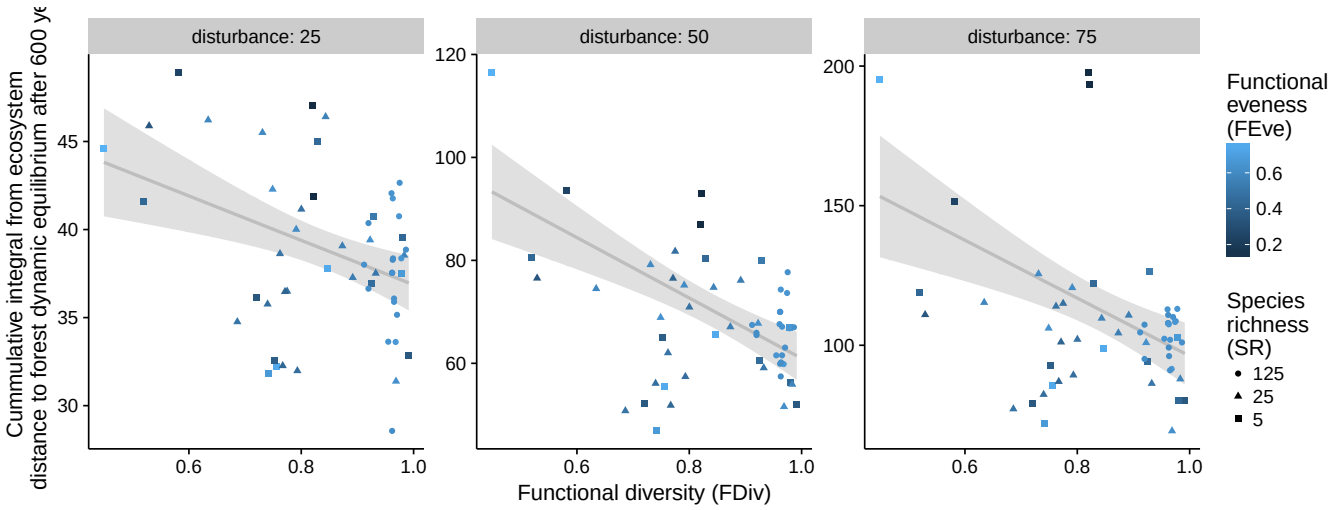

Figure 4: Ecosystem resilience after 600 years with taxonomic and functional diversity for different levels of disturbance. Cummulative integral from ecosystem distance to forest dynamic equilibrium after 600 years was represented against functional diversity [FDiv, Villéger et al., 2008] for different level of disturbance (25, 50 and 75% of total basal area); dot shapes represents the species richness whereas dot color represents functional eveness [FEve, Villéger et al., 2008].

Biodiversity effect

We measured all ecosystem outputs biodiversity net effect in disturbance simulations by comparing theim to their species corresponding monoculture simulations. The net effect was then partition between selection and complementarity effect. We normalized treatments effect by control net effect (see Table 2) to measure their aboveground biomass resilience to disturbance (see Figure 5). We found that complementarity effect was recovering net effect in the first decades untill it disappeared after a century. On the contrary selection effect was reduced or even removed by the disturbance. It increased during the whole simulation and was greater than complementarity effect only after decades. The time lag for which complementarity effect was non null and greater than selection effect was increasing with disturbance intensity. Finally 600 years after the disturbance event biodiversity net effect was still not recovered for a disturbance intensity greater than 25% of

basal area. We obtained those results for aboveground biomass. We found similar results but with an amlified signal for basal area (BA) and stem abundance (N but with an inverted signal because of the forest self thinning) (see Appendix 5: Disturbance simulations). Finally, forest growth primary productivity (GPP) recovered in few years (proportionnaly to disturbance), and its net effect was maintained by complementarity effect (see Appendix 5: Disturbance simulations).

Table 2: Table 1: Biodiversity net effect mean value and standard deviation for different ecosystem variable.

variable	mean	standard deviation	name	unit
agb	32.721	17.839	aboveground biomass	$tonC.ha^{-1}$
ba	1.633	0.743	basal area	$m^2.ha^{-1}$
n	103.880	231.623	number of stems	$n.ha^{-1}$
n10	-6.815	13.003	number of stems above 10cm dbh	$n.ha^{-1}$
gpp	0.147	0.047	growth primary production	$MgC.ha^{-1}$
npp	-0.041	0.036	net primary production	$MgC.ha^{-1}$
Rday	0.046	0.018	autotrophic respiration during day	$MgC.ha^{-1}$
Rnight	0.074	0.030	autotrophic respiration during night	$MgC.ha^{-1}$

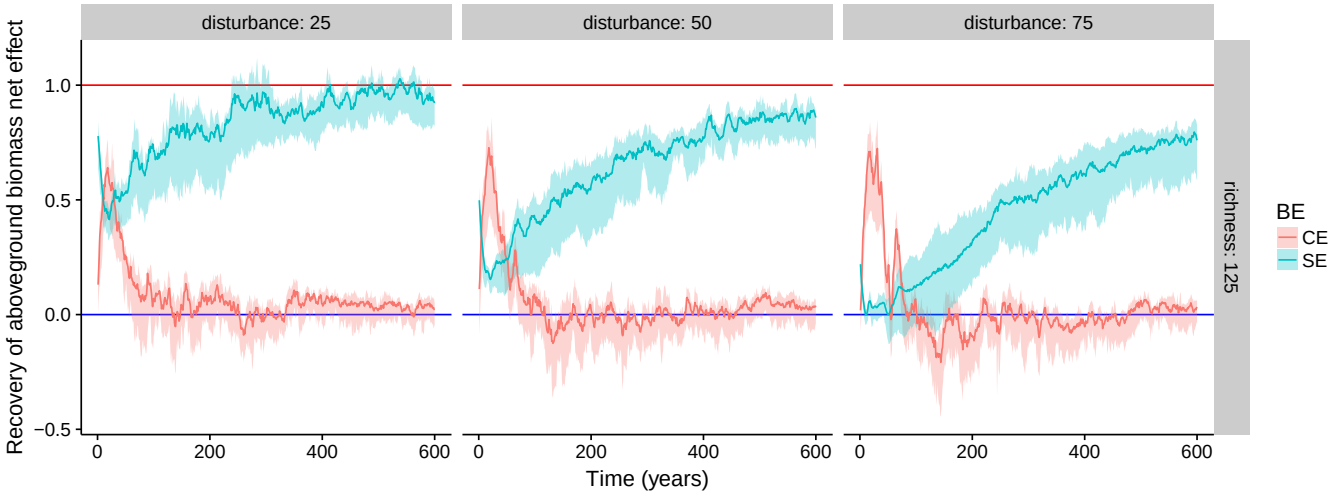

Figure 5: Resilience of complementarity and selection effects. Complementarity effect (CE) and selection effect (SE) where normalized by control net effect (NEc), thus measuring their resilience over time.

Sylviculture

Discussion

Appendix 1: TROLL model

I this Appendix we further detail modules of TROLL model.

Abiotic environment

A voxel space, with a resolution of 1 m^3, is used to explicilty model the abiotic environment. For each tree crown, leaf area density is calculated on tree geometry assuming a uniform distriution across voxels occupied by the crown. Leaf area density is computed within each voxel summing all tree crowns inside the voxel v, and is denoted $LAD(v)$ (leaf area per voxel in $mš.m^{-3}$). The vertical sum of LAD from voxel v to the ground level defines $LAI(v)$ (leaf area per fround area in $m^2.m^{-2}$ commonly called leaf area index):

$$LAI(v) = \sum_{v'=v}^{\infty} LAD(v') \tag{8}$$

Daily variations in light intensity (photosynthetic photon flux density PPFD in $\mu mol_{photons}.m^{-2}.s^{-1}$), temperature (T in degrees Celsius), and vapor pressure deficit (VPD in kPA) are computed to assess carbon assimilation within each voxel of the canopy and for a representative day per month (see Appendix 1 from Maréchaux and Chave for further details). Variation of PPFD Within the canopy is calculated as a loacal Beer-Lambert extinction law:

$$PPFD_{max,month}(v) = PPFD_{top,max,month} * e^{-k*LAI(v)} \tag{9}$$

The daily maximum incident PPFD at the top of canopy $PPFD_{top,max,month}$ is given as input. The extinction rate k is assumed as constant, besides is variation with zenith angle and species leaf inclination angle [Meir et al., 2000]. Moreover only vertical light diffusion is considered ignoring lateral light diffusion, which can have an important role especially in logging gaps. Finally, intra-day variation at half hour time steps t for a representative day every month are used to compute $PPFD_{month}(v,t)$, $T_{month}(v,t)$ and $VPD_{month}(v,t)$. Water and nutrient process both in soil and inside trees are not simulated.

Photosynthesis

Theory

Troll simulates the carbon uptake of each individual with the Farquhar, von Caemmerer and Berry model of C3 photosynthesis [Farquhar et al., 1980]. Gross carbon assimilation rate (A in

$\mu mol\ CO_2.m^{-2}.s^{-1}$) will be the minimum of eiter Rubisco activity (A_v) or RuBP generation (A_j):

$$A = min(A_v, A_j) \mid A_v = V_{cmax} * \frac{c_i - \Gamma^*}{c_i + K_m}\ ;\ A_j = \frac{J}{4} * \frac{c_i - \Gamma^*}{c_i + 2 * \Gamma^*} \tag{10}$$

V_{cmax} is the maximum rate of carboxylation ($\mu mol\ CO_2.m^{-2}.s^{-1}$). c_i is the CO_2 partial pressure at carboxylation sites. Γ^* is the CO_2 compensation point in absence of dark respiration. K_m is the apparent knietic constant of the Rubisco. And J is the electron transport rate ($\mu mole^-.m^{-2}.s^{-1}$). J depends on the light intensity with $PPFD$:

$$J = \frac{1}{2 * \theta} * [\alpha * PPFD + J_{max} - \sqrt{(\alpha * PPFD + J_{max})^2 - 4 * \theta * \alpha * PPFD * J_{max}}] \tag{11}$$

J_{max} is the maximal electron transport capacity ($\mu mole^-.m^{-2}.s^{-1}$). θ is the curvature factor. And α is the apparent quantum yield to electron transport ($mole^-.mol\ photons^{-1}$).

Carbon assimilation by photosynthesis will then be limited by the CO_2 partial pressure at carboxylation sites. Stomata controls the gas concentration at carboxylation sites throught stomatal transport:

$$A = g_s * (c_a - c_i) \tag{12}$$

g_s is the stomatal conductance to CO_2 ($molCO_2.m^{-2}.s^{-1}$). TROLL simulates stomatal conductance g_s with the model from [Medlyn et al., 2011]:

$$g_s = g_0 + (1 + \frac{g_1}{\sqrt{VPD}}) * \frac{A}{c_a} \tag{13}$$

g_0 and g_1 are parameters from the model. TROLL model assume $g_0 \approx 0$ (empirically tested and considered as reasonable).

Parametrization

Leaf traits can be used as proxy of photosynthesis, especially leaf nutrient content which directly play a role in it [Wright et al., 2004]. Domingues et al. [2010] suggested that V_{cmac} and J_{max} were both limited by the leaf concentration of nitrogen N and phosphorus P ($mg.g^{-1}$):

$$log_{10}V_{cmax-M} = min(\begin{array}{l} -1.56 + 0.43 * log_{10}N - 0.37 * log_{10}LMA \\ -0.80 + 0.45 * log_{10}P - 0.25 * log_{10}LMA \end{array}) \tag{14}$$

$$log_{10}J_{max-M} = min(\begin{array}{l} -1.50 + 0.41 * log_{10}N - 0.45 * log_{10}LMA \\ -0.74 + 0.44 * log_{10}P - 0.32 * log_{10}LMA \end{array}) \tag{15}$$

V_{cmax-M} and J_{max-M} are the photosynthetic capacities at $25°C$ of mature leaves per leaf dry mass (resp. $\mu molCO_2.g^-1.s^{-1}$ and $\mu mole^-.g^{-1}.s^{-1}$). LMA is the leaf mass per are ($g.cm^{-2}$). V_{cmax} and J_{max} are calculated by multiplying V_{cmax-M} and J_{max-M} by LMA. V_{cmax} and J_{max} variation with temperature are caluclated with Bernacchi et al. [2003] (see Appendix 2 from Maréchaux and Chave for further details).

TROLL computes leaf carbon assimilation A_l combining equations from (10) to (15) for each tree crown voxel within in each crown layer l:

$$A_l = \frac{1}{n_v * t_M} * \sum_{v} \sum_{t=1}^{t_M} A(PPFD_{month}(v,t), VPD_{month}(v,t), T_{month}(v,t)) \tag{16}$$

$PPFD_{month}(v,t)$, $VPD_{month}(v,t)$, and $T_{month}(v,t)$ are derived from microclimatic data. n_v is the number of voxels within crown layer l. And the sum is calculated over the t_M half-hourly intervals t of a tipical day.

Autotrophic respiration

A large fraction of plants carbon uptake is actually used for plant maintenance and growth respiration. The autotrophic respiration can represents up to 65% of the gross primary productivity but varies strongly among species, sites, and environnements.

TROLL uses Atkin et al. [2015] database of mature leaf dark respiration and associated leaf traits to compute leaf maintenance respiration:

$$R_{leaf-M} = 8.5431 - 0.1306 * N - 0.5670 * P - 0.0137 * LMA + 11.1 * V_{cmax-M} + 0.1876 * N * P \tag{17}$$

R_{leaf-M} si the dark respiration rate per leaf dry mass at a temperaure of $25°C$ ($nmolCO_2.g^{-1}.s^{-1}$). The other terms are in equations (14) and (15). TROLL assume leaf respiration during day light to be 40% of leaf dark respiration, and computes total leaf respiration by accounting for the legnth of daylight.

TROLL model stem respiration (R_{stem} in $\mu molC.s^{-1}$) with a constant respiration rate per volume of sapwood:

$$R_{stem} = 39.6 * \pi * ST * (dbh - ST) * (h - CD) \tag{18}$$

dbh, h, CD and ST are tree diameter at breast height, height, corwn depth and sapwoond thickness, respectively (m). TROLL assumes $ST = 0.04\ m$ when $dbh > 30\ cm$ and an increasing ST for lower dbh.

Finally, TROLL computes both fine root maintenance respiration, as half of the leaf maintenance respiration. Whereas coarse root and branch maintenance respiration is computed as half of the stem respiration. And growth respiration (R_{growth}) is assumed to account for 25% of the gross primary productivity minus the sum of maintenance respirations.

Net carbon uptake

Net primary production of carbon for one individual NPP_{ind} (gC) is computed by the balance between gross primary production GPP_{ind} and respirations R:

$$NPP_{ind} = GPP_{ind} - R_{maintenance} - R_{growth} \tag{19}$$

TROLL partitions individuals total leaf area LA into three pools for different leaf age classes corresponding to different photosynthesis efficiency (young, mature and old leaves with LA_{young}, LA_{mature}, and LA_{old} respectivelly). Consequently we can compute growth primary production for one individual as:

$$GPP_{ind} = 189.3 * \Delta t * \sum_{l=\lfloor h-CD \rfloor+1}^{\lfloor h \rfloor} [A_l] * (\frac{LA_{young}}{2} + LA_{mature} + \frac{LA_{old}}{2}) \tag{20}$$

h and CD are tree height and crown depth, repectivelly (m). $\lfloor x \rfloor$ is the rounding function. Δt is the duration of a timestep ($year$).

Thus, TROLL can compute carbon allocation to wood into an increment of stem volume ΔV (m^3):

$$\Delta V = 10^{-6} * \frac{f_{wood} * NPP_{ind}}{0.5 * wsg} * Senesc(dbh) \tag{21}$$

f_{wood} is the fixed fraction of NPP allocated to stem and branches. wsg is the wood specific gravity ($g.cm^{-3}$, see 1). TROLL assume large trees less efficient to convert NPP as growth by using a size-related growth decline with function $Senesc$ after a specific diameter at brest height threshold dbh_{thresh}:

$$Senesc(dbh) = max(0; 3 - 2 * \frac{dbh}{dbh_{thresh}}) \tag{22}$$

Finally, TROLL can compute carbon allocation to canopy with canopy NPP fraction denoted f_{canopy} and decomposed into leaf, twig and fruit production. Carbon allocation to leaf results in a new young leaf pool, whereas other leaf pools are updated as follow:

$$\begin{aligned} \Delta LA_{young} &= \frac{2*f_{leaves}*NPP_{ind}}{LMA} - \frac{LA_{young}}{\tau_{young}} \\ \Delta LA_{mature} &= \frac{LA_{young}}{\tau_{young}} - \frac{LA_{mature}}{\tau_{mature}} \\ \Delta LA_{old} &= \frac{LA_{mature}}{\tau_{mature}} - \frac{LA_{old}}{\tau_{old}} \end{aligned} \tag{23}$$

τ_{young}, τ_{mature}, and τ_{old} are species residence times in each leaf pools ($years$). The sum of residency time thus defined the leaf lifespan $LL = \tau_{young} + \tau_{mature} + \tau_{old}$ ($years$). τ_{young} is set to one month and τ_{mature} is set to a third of leaf lifespan LL. Belowground carbon allocation is not simulated inside TROLL.

Tree growth

Once the increment of stem volume ΔV calculated with equation (21), TROLL convert it into an increment of tree diameter at breast height denoted Δdbh. TROLL infer tree height from dbh using a Michaelis-Menten equation:

$$h = h_{lim} * \frac{dbh}{dbh + a_h} \tag{24}$$

On the other hand, we have the trunk volume $V = C * \pi * (\frac{dbh}{2})^2 * h$, thus:

$$\begin{aligned} \Delta V &= C * \tfrac{1}{2} * \pi * h * dbh * \Delta dbh + C * \pi * (\tfrac{dbh}{2})^2 * h \\ \Delta V &= V * \tfrac{\Delta dbh}{dbh} * (3 - \tfrac{dbh}{dbh + ah}) \end{aligned} \tag{25}$$

Next, TROLL used the new trunk dimension (dbh and h) to update tree crown geometry using allometric equations [Chave et al., 2005]:

$$\begin{aligned} CR &= 0.80 + 10.47 * dbh - 3.33 * dbh^2 \\ CD &= -0.48 + 0.26 * h \ ; \ CD = 0.13 + 0.17 * h \ (h < 5 \ m) \end{aligned} \tag{26}$$

Finally, TROLL computes the mean leaf density within the crown (LD in $m^2.m^{-3}$) assuming a uniform distribution:

$$LD = \frac{LA_{young} + LA_{mature} + LA_{old}}{\pi * CR^2 * CD} \tag{27}$$

Mortality

Mortality is partitioned in three factors inside TROLL: background death d_b, treefall death d_t and negative density dependent death d_{NDD}. Because density dependent death d_{NDD} is still in development inside TROLL we did not used it, so we will not detail is computation.

Chave et al. [2009] advocated for a wood economics spectrum opposing fast growing light wood species species with high risk of mortality to slow growing dense wood species with reduced risk of mortality. Hence, background mortality is derived from wood specific gravity wsg inside TROLL:

$$d_b = m * (1 - \frac{wsg}{wsg_{lim}}) + d_n \tag{28}$$

m ($events.year^{-1}$) is the reference background death rate for lighter wood species (pioneers). d_n represents death by carbohydrates shortage. If the number of consecutive day with $NPP_{ind} < 0$ (19) is superior to tree leaf lifespan d_n is set to 1 and remains null in other cases.

Mortality by treefall inside TROLL depends on a specifric stochastic threshold θ:

$$\theta = h_{max} * (1 - v_T * |\zeta|) \tag{29}$$

h_{max} is the maximal tree height. v_T is the variance term set to 0.3. $|\zeta|$ is the absolute value of a random centered and scaled Gaussian. If the tree hieght h is superior to θ then the tree may fall with a probability $1 - \theta/h$ [Chave, 1999]. The treefall direction is random (drawn from a uniform law ($\mathcal{U}[0, 2\pi]$). All tree in the trajectory of the falling tree will be hurted through a variable denoted $hurt$, incremented by fallen tree height h. If a tree height is inferior than its $hurt$ values then it may die with a probability $1 - \frac{1}{2}\frac{h}{hurt}$. $hurt$ variable is reset to null at each timestep ($month$).

Recruitment

Once the tree became fertile they will start to disperse seeds. TROLL consider tree as fertile after a specific height threshold h_{mature} [Wright et al., 2005]:

$$h_{mature} = -11.47 + 0.90 * h_{max} \tag{30}$$

But TROLL is not considering seed directly through a seedbank, instead seed might be interpreted as a seedling recruitment opportunity. The number of reproduction opportunities per mature tree is denoted n_s and set to 10 for all species. This assumption originates from a trade-off between seed number and seed size resulting in equivalent survival and recruitment probability. All n_s events are dispersed with a distance randomly drawn from a Gaussian distribution. Additionally, TROLL model consider external seedrain through n_{ext} events of seed immigration:

$$n_{ext} = N_{tot} * f_{reg} * n_{ha} \tag{31}$$

N_{tot} is the external seedrain per hectare (number of reproduction opportunities). f_{reg} is the species regional frequency. n_{ha} is the simulated plot size in ha.

Finally, a bank of seedlings to be recruited is defined for each pixel. If the ground-level light reaches a species light compensation point LCP the species will be recruited:

$$LCP = \frac{R_{leaf}}{\phi} \tag{32}$$

R_{leaf} is the leaf respiration for maintenance (see (17)). ϕ is the quantum yield ($\mu molC.\mu mol\ photon$) set to 0.06. If several species reach their LCP, one is picked at random. Seedlings are recruited with following intial geometry:

$$\begin{aligned} dbh &= \tfrac{a_h}{h_{max}-1} \\ h &= 1\ m \\ CR &= 0.5\ m \\ CD &= 0.3\ m \\ LD &= 0.8\ m^2.^{-3} \end{aligned} \tag{33}$$

Appendix 2: Leaf lifespan model

TROLL model previous implementation encompass Reich's 1991 and 1997 and Wright's 2004 allometries to estimate leaf lifespan with [Reich et al., 1991, 1997, Wright et al., 2004]. But we have shown that Reich's allometries are underestimating leaf lifespan for low LMA species. Moreover simulations estimated unrealistically low aboveground biomass for low LMA species. We assumed Reich's allometries underestimation of leaf lifespan for low LMA species being the source of unrealistically low aboveground biomass inside TROLL simulations. We decided to find a better allometry with Wright et al. [2004] GLOPNET dataset.

Material and methods

We compiled functional traits from GLOPNET [Wright et al., 2004], TRY [Kattge et al., 2011], and DRYAD [Chave et al., 2009] databases (see 3). We kept dataset given by GLOPNET as origin dataset for observations. Dataset defined as origin corresponded to leaf lifespan (LL) and most of the time to leaf mass per area (LMA) and leaf nitrogen content per leaf dry mass ($Nmass$). We measured variable importance in functionnal traits to explain leaf lifespan with out-of bag method applied on a random forest. Then, we used a béayesian apporach to test different models with growing level of complexity. We retained the model with the best tradeoff between model complexity (number of parameters K), convergence, likelihood, and prediction quality (root mean sqaure error of prediciton $RMSEP$). We finally tested the new allometry obtained with the selected model with TROLL simulations.

Table 3: Functional traits gathered with TRY.

Name	Trait	Unit	TRYcode
LL	Leaf lifespan (longevity)	month	12
SLA	Leaf area per leaf dry mass (specific leaf area, SLA)	$m^2.kg^{-1}$	11
N	Leaf nitrogen (N) content per leaf dry mass	$mg.g^{-1}$	15
P	Leaf phosphorus (P) content per leaf dry mass	$mg.g^{-1}$	14
wsg	Stem dry mass per stem fresh volume (stem specific density)	$mg.mm^{-3}$	4

Results

Out of the bag method applied on a random forest highlighted the importance of leaf nitrogen content per leaf dry mass (N_m) to model leaf lifespan (see 4). N_m importance was higher than leaf mass per area (158 against 96 percent of mean square error increase) which was used as a proxy for leaf lifespan in previous models. Finally, wood specific gravity (wsg) add also a significant

importance in leaf lifespan estimation.

Table 4: Variable importance calculated with out-of the bag method applied on a random forest. First column represents the mean decrease in mean square error (%IncMSE) whereas second column represents the total decrease in node impurities, measured by the Gini Index (IncNodePurety). Leaf lifespan (LL) is taken in GLOPNET database from Wright et al. [2004]. Leaf mass per area (LMA), and leaf nitrogen content (Nmass) are taken both in TRY (https://www.try-db.org) and GLOPNET databases. Wood specific gravity (wsg) is taken both in TRY and DRYAD databases.

	%IncMSE	IncNodePurity
LMA	99.69390	2028.079
Nm	159.03360	2666.670
wsg	50.97284	1475.023

The selected model had a maximum likelihood of 13.6 and a RMSEP of 12 months:

$$LL_d \sim log\mathcal{N}(\beta_{1_d} * LMA - \beta_{2_d} * N * \beta_3 * wsg, \sigma) \tag{34}$$

Leaf lifespan LL follows a lognormal law with location infered from leaf lifespan LMA, nitrogen content N and wood specific gravity wsg and a scale σ. Each β_{i_d} is following a normal law located on β_i with a scale of σ_i. All β_i, σ_i, and σ are assumed without presemption following a gamma law. d represents the dataset random effects and encompass environmental and protocol variations.

Simulations are validating that this new allometry resolve the issue of unrealistically low aboveground biomass for low LMA species due to an early edath of individuals inside simulations. For instance with this allometry Symphonia sp 1 (a low LMA species) is now reaching a realistic aboveground biomass above 400 $tonC.ha^{-1}$ and realistic diameter and age distribution inside the final population.

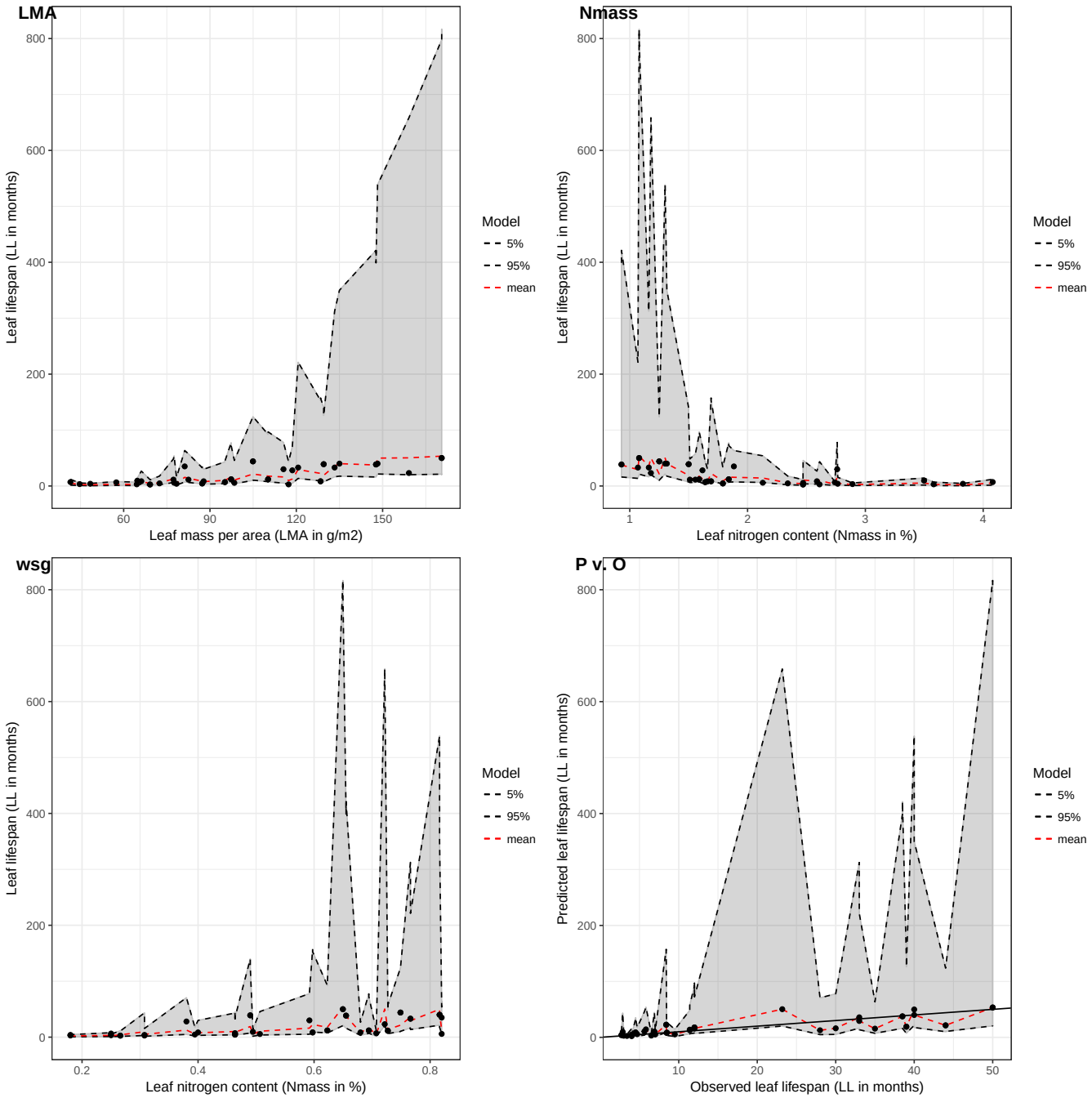

Figure 6: Leaflifespan predictions for the selected model with leaf mass per area (LMA), leaf nitrogen content (Nmass), wood specific gravity (wsg) and predicted versus observed values. Leaf lifespan (LL) is predicted with model M10 fit. Leaf mass per area (LMA) and leaf nitrogen content (Nmass), and wood specific gravity (wsg) are taken in a composite dataset of GLOPNET, TRY and DRYAD datasets.Warning LMA (resp. Nmass and wsg) is not constant and depend on the closest point value for right (resp. center and left) graph.

Appendix 3: Rotten tree model

In order to simulate sylviculture with TROLL we need to implement a new sylviculture module inside TROLL model code. A first litterature review was completed by an interview with Laurent Descroix of the Office Nationale des Forêts. We discovered that rotten trees were not random and seemed to depend both on tree species and diameter. This document presents modelling of relation between rotten trees and their species and diameter.

In fact we have two different questions:

- Predict if a tree will be probed as rotten (models **M**)
- Predict how much of tree volume is rotten (models **N**)

First all **M** model can be written as follow:

$$Rotten_n \sim \mathcal{B}(\theta_n), \quad n \in [1, N_{=3816}] \quad p \in [1, P_{=8}], \quad s \in [1, S_{=43}]$$

Secondly, all **N** models depend on a latent variable being the percentage of rotten wood Pt_r. We can assume that all trees are growing depending on species s and plot p fertility and are supposed to have a full healthy volume V_h for a given diameter dbh. We obtain following model:

$$V_f \sim \updownarrow\wr\}\mathcal{N}(V_h * Pt_r, \sigma), \quad n \in [1, N_{=3268}] \quad p \in [1, P_{=8}], \quad s \in [1, S_{=43}]$$

We retained following models :

Table 5: Models summary.

M	Model
$M_{s,p}$	$P_{rotten_n} \sim \mathcal{B}(inv_{logit}(\beta_0 + \beta_1 * dbh_n + \beta_{2_p} + \beta_{3_s}))$
$N_{s,p} + L_{s,p}$	$Volume_{of\ wood} \sim \updownarrow\wr\}\mathcal{N}(log[((\beta + \beta_p + \beta_s) * dbh^2) * (1 - Pr * ((\theta + \theta_p + \theta_s) * dbh^2))], \sigma)$

Probed rotten (M)

Based on complexity (number of parameters), convergence and likelihood we selected model $M_{p,s}$:

$M_{s,p}$: $P_{rotten_n} \sim \mathcal{B}(inv_{logit}(\beta_0 + \beta_1 * dbh_n + \beta_{2_p} + \beta_{3_s}))$

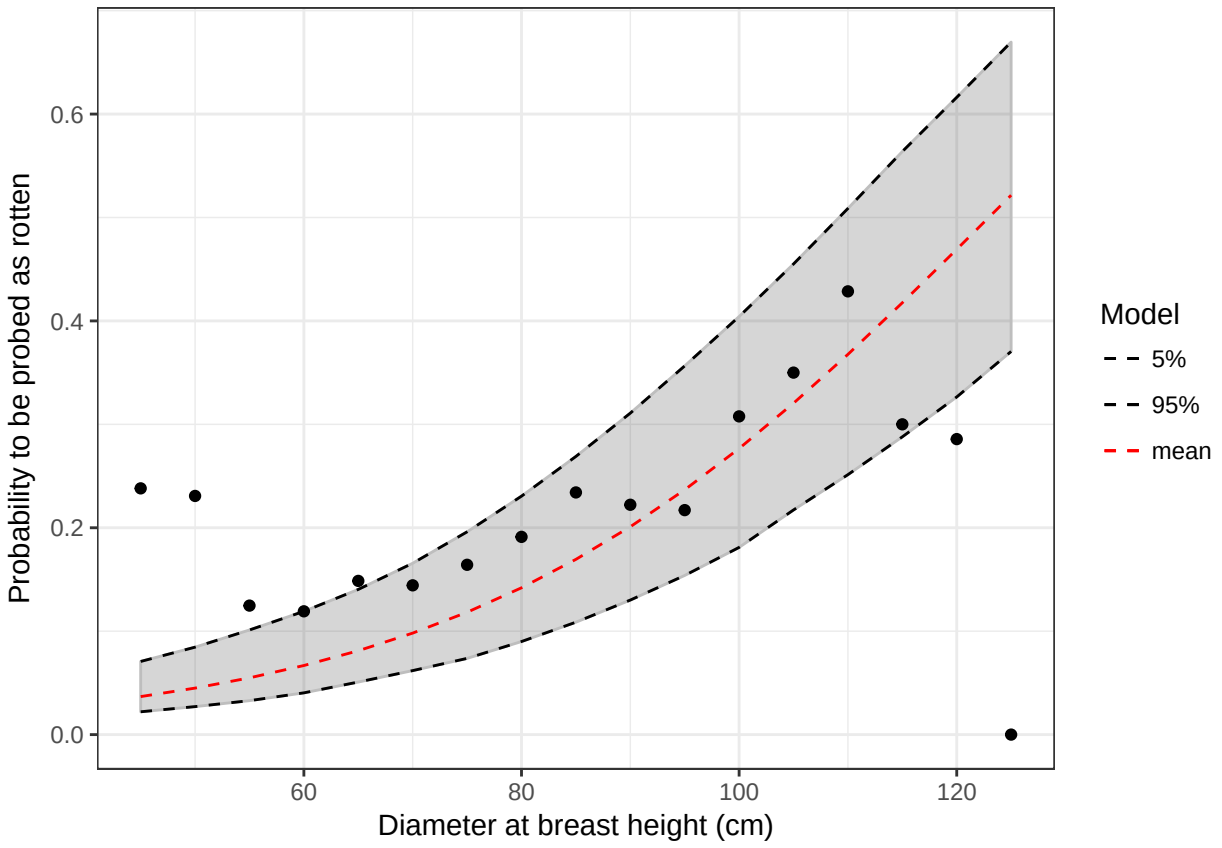

Table 6: Models prediction. Probability to be probed as rotten (P in %) for a given dbh (cm).

	45	50	55	60	65	70	75	80	85	90	95	100	105	110	115	120	125
P	4	4	5	7	8	10	12	14	17	20	24	28	32	37	42	47	52

Rotten volume (N)

Based on complexity (number of parameters), convergence and likelihood we selected model $N_{p,s}$ associated to hyperparameter ρ with model $L_{p,s}$:

$N_{s,p} + L_{s,p}$: $Volume_{of\ wood} \sim \updownarrow\wr\}\mathcal{N}(log[((\beta + \beta_p + \beta_s) * dbh^2) * (1 - Pr * ((\theta + \theta_p + \theta_s) * dbh^2))], \sigma)$

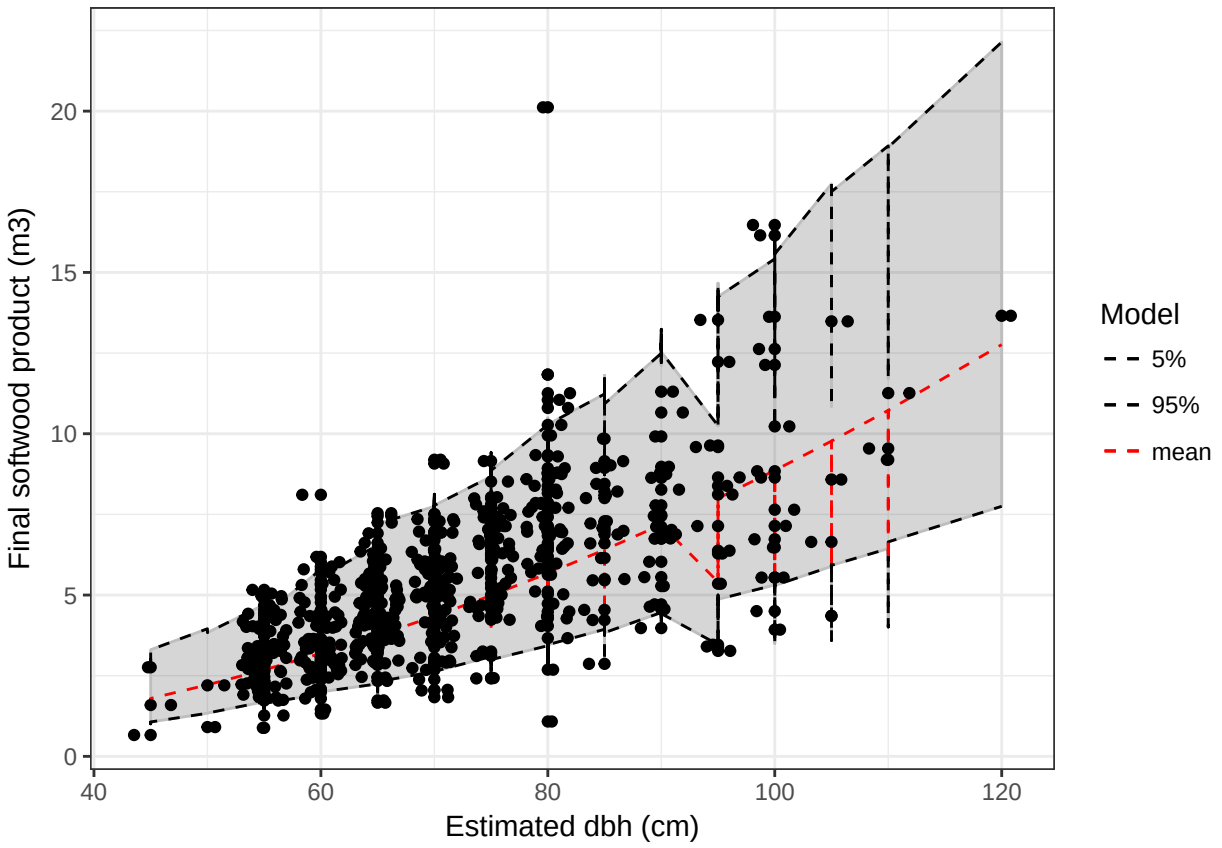

Table 7: Models prediction. Final volume of wood (V_f in m^3) and percent of rotten wood (V_p in %) for a given dbh (cm) if the tree was probed rotten.

	45	50	55	60	65	70	75	80	85	90	95	100	105	110	
Vf	1.66	2.02	2.39	2.78	3.18	3.58	3.98	4.37	4.74	5.09	5.41	5.68	5.9	6.06	
Vp	7.00	9.00	11.00	13.00	15.00	18.00	20.00	23.00	26.00	29.00	32.00	36.00	40.0	43.00	4

Appendix 4: Sensitivity analysis

Appendix 5: Disturbance simulations

Ecosystem functions

Appendix 4 presents ecosystem resilience after 600 years with taxonomic and functional diversity for different levels of disturbance. It encompass all functionnal diversity components [FRIC, FEve, FDiv, and FDis, Villéger et al., 2008]. And it presents results for both forest dynamic (Figure **??**) and forest production (Figure **??**).

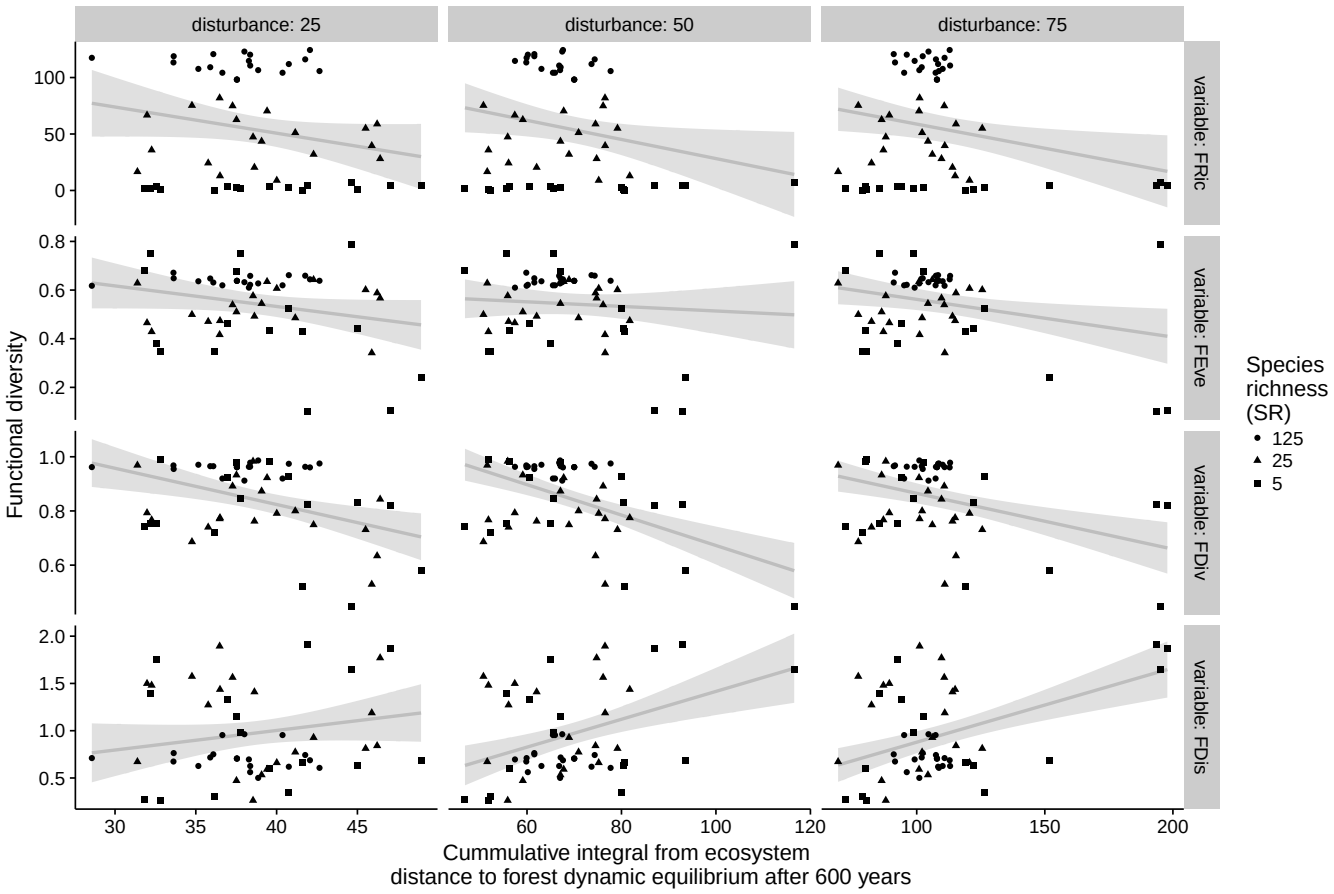

Figure 7: Ecosystem resilience after 600 years with taxonomic and functional diversity for different levels of disturbance. Cummulative integral from ecosystem distance to forest dynamic equilibrium after 600 years was represented against functional diversity [FRIC, FEve, FDiv, and FDis, Villéger et al., 2008] for different level of disturbance (25, 50 and 75% of total basal area); dot shapes represents the species richness.

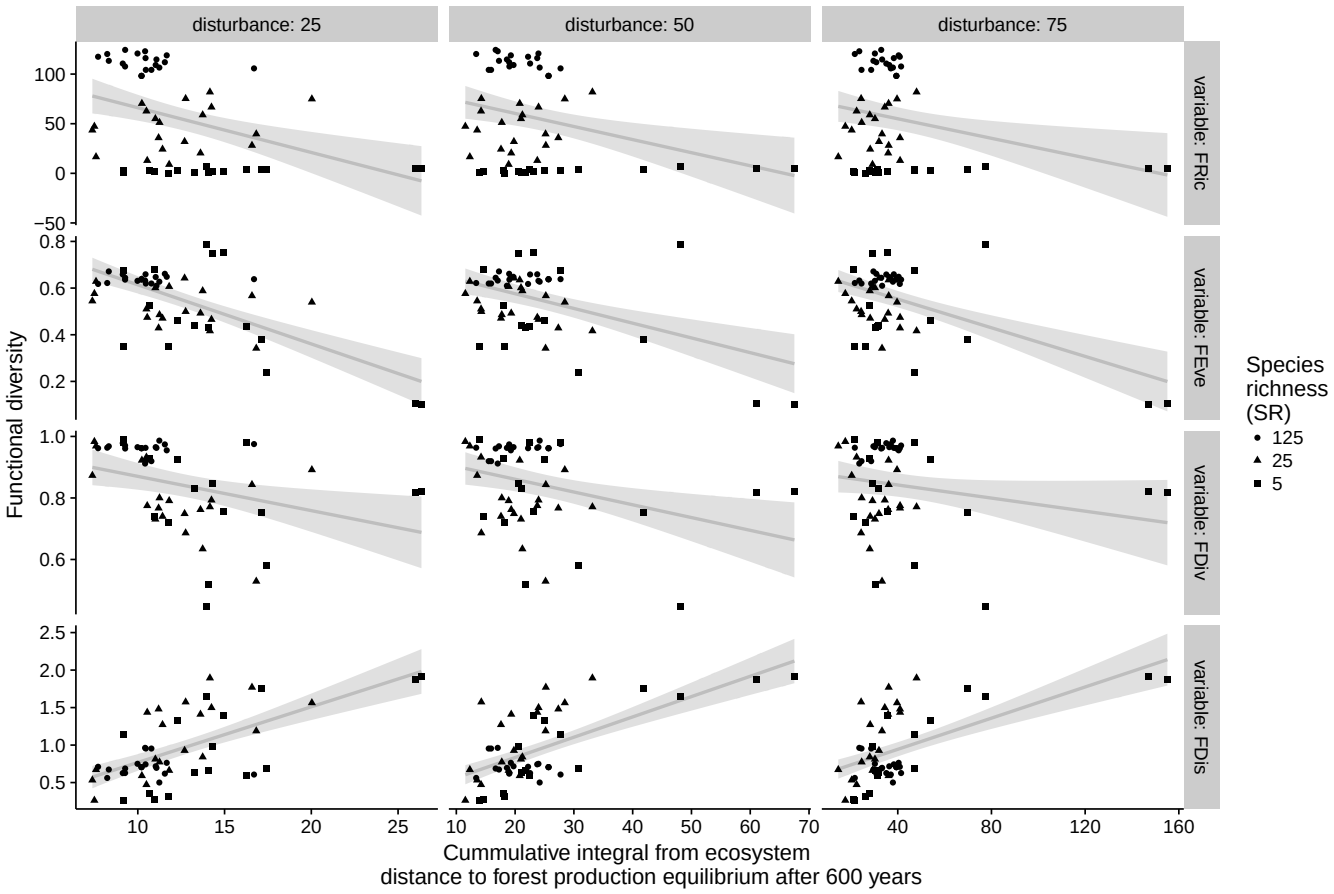

Figure 8: Ecosystem resilience after 600 years with taxonomic and functional diversity for different levels of disturbance. Cummulative integral from ecosystem distance to forest production equilibrium after 600 years was represented against functional diversity [FRIC, FEve, FDiv, and FDis, Villéger et al., 2008] for different level of disturbance (25, 50 and 75% of total basal area); dot shapes represents the species richness.

Biodiversity effect

Figure **??** presents the resilience of complementarity and selection effects for different ecosystem metrics (AGB, BA, N, GPP and NPP).

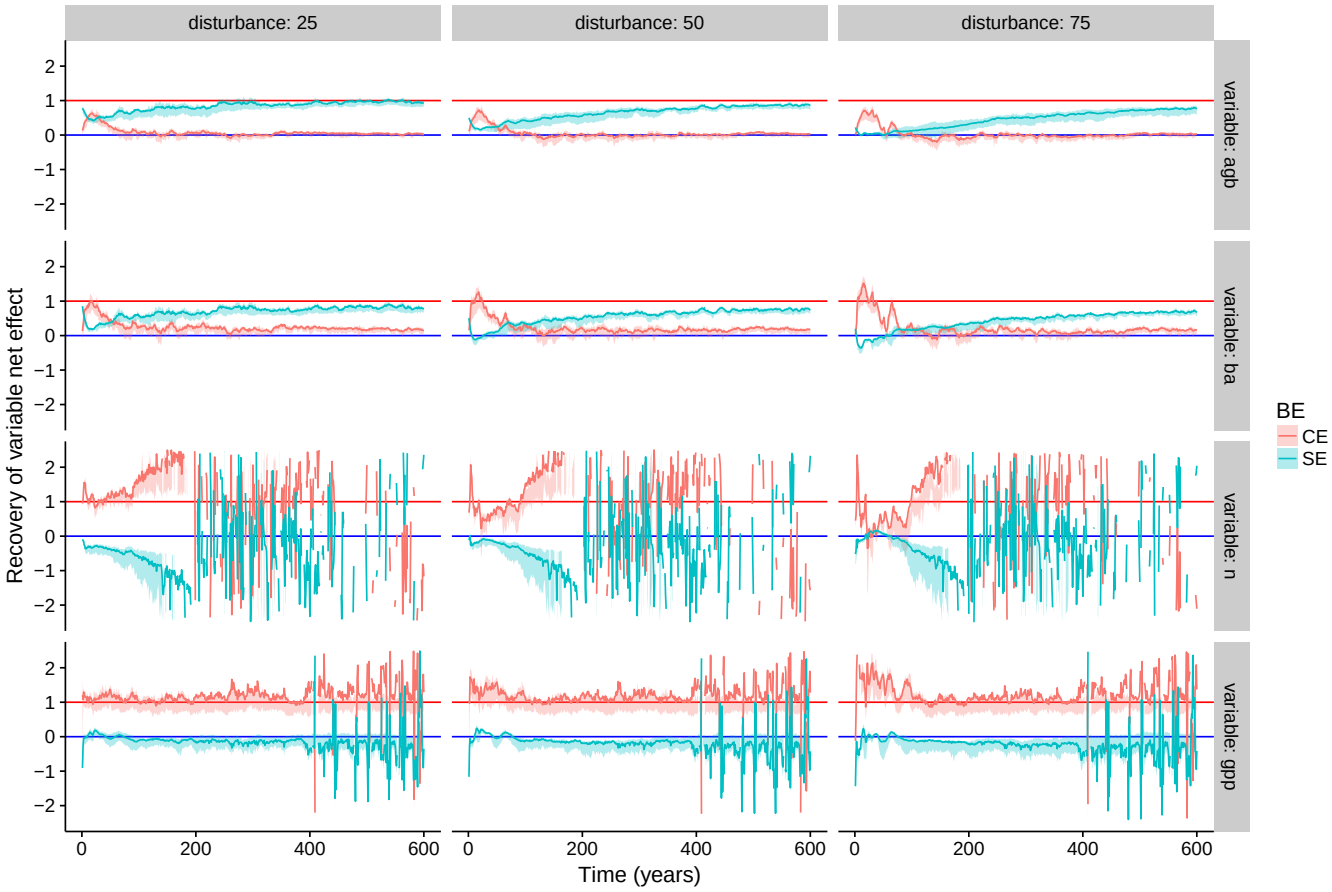

Figure 9: Resilience of complementarity and selection effects. Complementarity effect (CE) and selection effect (SE) where normalized by control net effect (NEc), thus measuring their resilience over time for different ecosystem variables (AGB, BA, N, GPP).

References

Owen K. Atkin, Keith J. Bloomfield, Peter B. Reich, Mark G. Tjoelker, Gregory P. Asner, Damien Bonal, Gerhard B??nisch, Matt G. Bradford, Lucas A. Cernusak, Eric G. Cosio, Danielle Creek, Kristine Y. Crous, Tomas F. Domingues, Jeffrey S. Dukes, John J G Egerton, John R. Evans, Graham D. Farquhar, Nikolaos M. Fyllas, Paul P G Gauthier, Emanuel Gloor, Teresa E. Gimeno, Kevin L. Griffin, Rossella Guerrieri, Mary A. Heskel, Chris Huntingford, Fran??oise Yoko Ishida, Jens Kattge, Hans Lambers, Michael J. Liddell, Jon Lloyd, Christopher H. Lusk, Roberta E. Martin, Ayal P. Maksimov, Trofim C. Maximov, Yadvinder Malhi, Belinda E. Medlyn, Patrick Meir, Lina M. Mercado, Nicholas Mirotchnick, Desmond Ng, ??lo Niinemets, Odhran S. O'Sullivan, Oliver L. Phillips, Lourens Poorter, Pieter Poot, I. Colin Prentice, Norma Salinas, Lucy M. Rowland, Michael G. Ryan, Stephen Sitch, Martijn Slot, Nicholas G. Smith, Matthew H. Turnbull, Mark C. Vanderwel, Fernando Valladares, Erik J. Veneklaas, Lasantha K. Weerasinghe, Christian Wirth, Ian J. Wright, Kirk R. Wythers, Jen Xiang, Shuang Xiang, and Joana Zaragoza-Castells. Global variability in leaf respiration in relation to climate, plant functional types and leaf traits. *New Phytologist*, 206(2):614–636, apr 2015. ISSN 14698137. doi: 10.1111/nph.13253. URL http://doi.wiley.com/10.1111/nph.13253.

Christopher Baraloto, C. E Timothy Paine, Lourens Poorter, Jacques Beauchene, Damien Bonal, Anne Marie Domenach, Bruno Hérault, Sandra Patiño, Jean Christophe Roggy, and Jerome Chave. Decoupled leaf and stem economics in rain forest trees. *Ecology Letters*, 13(11):1338–1347, 2010. ISSN 14610248. doi: 10.1111/j.1461-0248.2010.01517.x.

C. J. Bernacchi, C. Pimentel, and Stephen P. Long. In vivo temperature response functions of parameters required to model RuBP-limited photosynthesis. *Plant, Cell and Environment*, 26 (9):1419–1430, sep 2003. ISSN 01407791. doi: 10.1046/j.0016-8025.2003.01050.x. URL http://doi.wiley.com/10.1046/j.0016-8025.2003.01050.x.

J Blaser, A Sarre, D Poore, and S Johnson. No Title. *International Tropical Timber Organization, Yokohoma, Japan*, 2011.

Harald Bugmann. A review of forest gap models. *Climatic Change*, 51(3-4):259–305, 2001. ISSN 01650009. doi: 10.1023/A:1012525626267.

Geovana Carreño-Rocabado, Marielos Peña-Claros, Frans Bongers, Alfredo Alarcón, Juan Carlos Licona, and Lourens Poorter. Effects of disturbance intensity on species and functional diversity in a tropical forest. *Journal of Ecology*, 100(6):1453–1463, 2012. ISSN 00220477. doi: 10.1111/j.1365-2745.2012.02015.x.

J. Chave, C. Andalo, S. Brown, M. A. Cairns, J. Q. Chambers, D. Eamus, H. Fölster, F. Fromard, N. Higuchi, T. Kira, J. P. Lescure, B. W. Nelson, H. Ogawa, H. Puig, B. Riéra, and T. Yamakura. Tree allometry and improved estimation of carbon stocks and balance in tropical forests. *Oecologia*, 145(1):87–99, aug 2005. ISSN 00298549. doi: 10.1007/s00442-005-0100-x. URL http://link.springer.com/10.1007/s00442-005-0100-x.

Jérôme Chave. Study of structural, successional and spatial patterns in tropical rain forests using TROLL, a spatially explicit forest model. *Ecological Modelling*, 124(2-3):233–254, 1999. ISSN 03043800. doi: 10.1016/S0304-3800(99)00171-4.

Jerome Chave, David Coomes, Steven Jansen, Simon L Lewis, Nathan G Swenson, and Amy E Zanne. Towards a worldwide wood economics spectrum. *Ecology Letters*, 12(4):351–366, 2009. ISSN 1461023X, 14610248. doi: 10.1111/j.1461-0248.2009.01285.x. URL http://doi.wiley.com/10.1111/j.1461-0248.2009.01285.x.

Joseph H Connell. Diversity in tropical rain forests and coral reefs. *Science*, 199(4335):1302–1310, 1978. URL http://www.colby.edu/reload/biology/BI358j/Readings/Diversityinrainforestsandcoralreefs.pdf.

Angela Luciana de Avila, Ademir Roberto Ruschel, João Olegário Pereira de Carvalho, Lucas Mazzei, José Natalino Macedo Silva, José do Carmo Lopes, Maristela Machado Araujo, Carsten F. Dormann, and Jürgen Bauhus. Medium-term dynamics of tree species composition in response to silvicultural intervention intensities in a tropical rain forest. *Biological Conservation*, 191:577–586, 2015. ISSN 00063207. doi: 10.1016/j.biocon.2015.08.004. URL http://dx.doi.org/10.1016/j.biocon.2015.08.004.

Tomas Ferreira Domingues, Patrick Meir, Ted R. Feldpausch, Gustavo Saiz, Elmar M. Veenendaal, Franziska Schrodt, Michael Bird, Gloria Djagbletey, Fidele Hien, Halidou Compaore, Adama Diallo, John Grace, and Jon Lloyd. Co-limitation of photosynthetic capacity by nitrogen and phosphorus in West Africa woodlands. *Plant, Cell and Environment*, 33(6):959–980, jan 2010. ISSN 01407791. doi: 10.1111/j.1365-3040.2010.02119.x. URL http://doi.wiley.com/10.1111/j.1365-3040.2010.02119.x.

G. D. Farquhar, S. von Caemmerer, and J. A. Berry. A biochemical model of photosynthetic CO2 assimilation in leaves of C3 species. *Planta*, 149(1):78–90, jun 1980. ISSN 00320935. doi: 10.1007/BF00386231. URL http://link.springer.com/10.1007/BF00386231.

Rico Fischer, Friedrich Bohn, Mateus Dantas de Paula, Claudia Dislich, J??rgen Groeneveld, Alvaro G. Guti??rrez, Martin Kazmierczak, Nikolai Knapp, Sebastian Lehmann, Sebastian Paulick, Sandro P??tz, Edna R??dig, Franziska Taubert, Peter K??hler, and Andreas Huth. Lessons learned from applying a forest gap model to understand ecosystem and carbon dynamics of complex tropical forests. *Ecological Modelling*, 326:124–133, 2016. ISSN 03043800. doi: 10.1016/j.ecolmodel.2015.11.018. URL http://www.sciencedirect.com/science/article/pii/S0304380015005505.

Luke Gibson, Tien Ming Lee, Lian Pin Koh, Barry W. Brook, Toby A. Gardner, Jos Barlow, Carlos A. Peres, Corey J. A. Bradshaw, William F. Laurance, Thomas E. Lovejoy, and Navjot S. Sodhi. Corrigendum: Primary forests are irreplaceable for sustaining tropical biodiversity. *Nature*, 505(7485):710–710, 2013. ISSN 0028-0836. doi: 10.1038/nature12933. URL http://www.nature.com/doifinder/10.1038/nature12933.

J-M Guehl, D Bonal, A Ferhi, T S Barigah, G Farquhar, a B T Ecology Granier, and Management of a Neotropical Rainforest. *Ecology and Management of a Neotropical Rainforest*. Elsevier, 2004. ISBN 2842994558. URL http://agritrop.cirad.fr/522004/.

Devanandham Henry and Jose Emmanuel Ramirez-Marquez. Generic metrics and quantitative approaches for system resilience as a function of time. *Reliability Engineering and System Safety*, 99:114–122, 2012. ISSN 09518320. doi: 10.1016/j.ress.2011.09.002. URL http://www.sciencedirect.com/science/article/pii/S0951832011001748.

Bruno Herault, Julia Ouallet, Lilian Blanc, Fabien Wagner, and Christopher Baraloto. Growth responses of neotropical trees to logging gaps. *Journal of Applied Ecology*, 47(4):821–831, 2010. ISSN 00218901. doi: 10.1111/j.1365-2664.2010.01826.x.

Andreas Huth, Martin Drechsler, and Peter Köhler. Multicriteria evaluation of simulated logging scenarios in a tropical rain forest. *Journal of Environmental Management*, 71(4):321–333, 2004. ISSN 03014797. doi: 10.1016/j.jenvman.2004.03.008. URL http://www.sciencedirect.com/science/article/pii/S0301479704000568.

J. Kattge, S. Diaz, S. Lavorel, I. C. Prentice, P. Leadley, G. B??nisch, E. Garnier, M. Westoby, P. B. Reich, I. J. Wright, J. H C Cornelissen, C. Violle, S. P. Harrison, P. M. Van Bodegom, M. Reichstein, B. J. Enquist, N. A. Soudzilovskaia, D. D. Ackerly, M. Anand, O. Atkin, M. Bahn, T. R. Baker, D. Baldocchi, R. Bekker, C. C. Blanco, B. Blonder, W. J. Bond, R. Bradstock, D. E. Bunker, F. Casanoves, J. Cavender-Bares, J. Q. Chambers, F. S. Chapin, J. Chave, D. Coomes, W. K. Cornwell, J. M. Craine, B. H. Dobrin, L. Duarte, W. Durka, J. Elser, G. Esser, M. Estiarte, W. F. Fagan, J. Fang, F. Fern??ndez-M??ndez, A. Fidelis, B. Finegan, O. Flores, H. Ford, D. Frank, G. T. Freschet, N. M. Fyllas, R. V. Gallagher, W. A. Green, A. G. Gutierrez, T. Hickler, S. I. Higgins, J. G. Hodgson, A. Jalili, S. Jansen, C. A. Joly, A. J. Kerkhoff, D. Kirkup, K. Kitajima, M. Kleyer, S. Klotz, J. M H Knops, K. Kramer, I. K??hn, H. Kurokawa, D. Laughlin, T. D. Lee, M. Leishman, F. Lens, T. Lenz, S. L. Lewis, J. Lloyd, J. Llusi??, F. Louault, S. Ma, M. D. Mahecha, P. Manning, T. Massad, B. E. Medlyn, J. Messier, A. T. Moles, S. C. M??ller, K. Nadrowski, S. Naeem, ?? Niinemets, S. N??llert, A. N??ske, R. Ogaya, J. Oleksyn, V. G. Onipchenko, Y. Onoda, J. Ordo??ez, G. Overbeck, W. A. Ozinga, S. Pati??o, S. Paula, J. G. Pausas, J. Pe??uelas, O. L. Phillips, V. Pillar, H. Poorter, L. Poorter, P. Poschlod, A. Prinzing, R. Proulx, A. Rammig, S. Reinsch, B. Reu, L. Sack, B. Salgado-Negret, J. Sardans, S. Shiodera, B. Shipley, A. Siefert, E. Sosinski, J. F. Soussana, E. Swaine, N. Swenson, K. Thompson, P. Thornton, M. Waldram, E. Weiher, M. White, S. White, S. J. Wright, B. Yguel, S. Zaehle, A. E. Zanne, and C. Wirth. TRY - a global database of plant traits. *Global Change Biology*, 17(9):2905–2935, sep 2011. ISSN 13652486. doi: 10.1111/j.1365-2486.2011.02451.x. URL http://doi.wiley.com/10.1111/j.1365-2486.2011.02451.x.

Peter Köhler and Andreas Huth. The effects of tree species grouping in tropical rainforest modelling: Simulations with the individual-based model FORMIND. *Ecological Modelling*, 109(3):301–321, 1998. ISSN 03043800. doi: 10.1016/S0304-3800(98)00066-0. URL http://www.sciencedirect.com/science/article/pii/S0304380098000660.

Peter Köhler and Andreas Huth. Simulating growth dynamics in a South-East Asian rainforest threatened by recruitment shortage and tree harvesting. *Climatic Change*, 67(1):95–117, nov 2004. ISSN 0165-0009. doi: 10.1007/s10584-004-0713-9. URL http://link.springer.com/10.1007/s10584-004-0713-9.

Simon L. Lewis, Malhi Yadvinder, and Phillips Oliver L. Fingerprinting the impacts of global change on tropical forests. *Philosophical Transactions: Biological Sciences*, 359(1443):437–462, 2004. ISSN 0962-8436. doi: 10.1098/rstb.2003.1432. URL http://rstb.royalsocietypublishing.org/content/359/1443/437.shorthttp://www.jstor.org/stable/4142193.

M Loreau. Biodiversity and ecosystem functioning: recent theoretical advances. *Oikos*, 91 (May):3–17, 2000. ISSN 1600-0706. doi: doi:10.1034/j.1600-0706.2000.910101.x. URL http://onlinelibrary.wiley.com/doi/10.1034/j.1600-0706.2000.910101.x/full.

M Loreau and a Hector. Partitioning selection and complementarity in biodiversity experiments. *Nature*, 412(6842):72–6, 2001. ISSN 0028-0836. doi: 10.1038/35083573. URL http://www.ncbi.nlm.nih.gov/pubmed/11452308.

Michel Loreau. Linking biodiversity and ecosystems: towards a unifying ecological theory. *Philosophical transactions of the Royal Society of London. Series B, Biological sciences*, 365(1537):49–60, 2010. ISSN 1471-2970. doi: 10.1098/rstb.2009.0155. URL http://apps.webofknowledge.com/full_record.do?product=WOS&search_mode=CitingArticles&qid=7&SID=V1TwrrLNJKUhYkGvYOi&page=10&doc=91&cacheurlFromRightClick=no.

Isabelle Maréchaux and Jérôme Chave. Joint simulation of carbon and tree diversity in an Amazonian forest with an individual-based forest model. *Inprep*, pages 1–13.

Philip A. Martin, Adrian C. Newton, Marion Pfeifer, Min Sheng Khoo, and James M. Bullock. Impacts of tropical selective logging on carbon storage and tree species richness: A meta-analysis. *Forest Ecology and Management*, 356:224–233, 2015. ISSN 03781127. doi: 10.1016/j.foreco.2015.07.010. URL http://dx.doi.org/10.1016/j.foreco.2015.07.010.

Belinda E. Medlyn, Remko A. Duursma, Derek Eamus, David S. Ellsworth, I. Colin Prentice, Craig V M Barton, Kristine Y. Crous, Paolo De Angelis, Michael Freeman, and Lisa Wingate. Reconciling the optimal and empirical approaches to modelling stomatal conductance. *Global Change Biology*, 17(6):2134–2144, jun 2011. ISSN 13541013. doi: 10.1111/j.1365-2486.2010.02375.x. URL http://doi.wiley.com/10.1111/j.1365-2486.2010.02375.x.

Patrick Meir, John Grace, and Antonio C. Miranda. Photographic method to measure the vertical distribution of leaf area density in forests. *Agricultural and Forest Meteorology*, 102(2-3):105–111, 2000. ISSN 01681923. doi: 10.1016/S0168-1923(00)00122-2. URL http://www.sciencedirect.com/science/article/pii/S0168192300001222.

Oyomoare L. Osazuwa-Peters, Iván Jiménez, Brad Oberle, Colin A. Chapman, and Amy E. Zanne. Selective logging: Do rates of forest turnover in stems, species composition and functional traits decrease with time since disturbance? - A 45 year perspective. *Forest Ecology and Management*,

357:10–21, 2015. ISSN 03781127. doi: 10.1016/j.foreco.2015.08.002. URL http://dx.doi.org/10.1016/j.foreco.2015.08.002.

Stephen W. Pacala, Charles D. Canham, John Saponara, John A. Silander, Richard K. Kobe, and Eric Ribbens. Forest models defined by field measurements: estimation, error analysis and dynamics. *Ecological Monographs*, 66(1):1–43, feb 1996. ISSN 00129615. doi: 10.2307/2963479. URL http://doi.wiley.com/10.2307/2963479.

Rémi Perrone, François Munoz, Benjamin Borgy, Xavier Reboud, and Sabrina Gaba. How to design trait-based analyses of community assembly mechanisms: insights and guidelines from a literature review. *Journal of PPEES Sources*, 25:29–44, 2017. ISSN 1433-8319. doi: 10.1016/j.ppees.2017.01.004. URL http://dx.doi.org/10.1016/j.ppees.2017.01.004.

P. B. Reich, C. Uhl, M. B. Walters, and D. S. Ellsworth. Leaf lifespan as a determinant of leaf structure and function among 23 amazonian tree species. *Oecologia*, 86(1):16–24, mar 1991. ISSN 00298549. doi: 10.1007/BF00317383. URL http://link.springer.com/10.1007/BF00317383.

Peter B Reich, Michael B Walters, and David S Ellsworth. From tropics to tundra: Global convergence in plant functioning. *Ecology*, 94(December):13730–13734, 1997. ISSN 0027-8424. doi: 10.1073/pnas.94.25.13730.

Nadja Rüger, Guadalupe Williams-Linera, W. Daniel Kissling, and Andreas Huth. Long-Term Impacts of Fuelwood Extraction on a Tropical Montane Cloud Forest. *Ecosystems*, 11(6):868–881, sep 2008. ISSN 1432-9840. doi: 10.1007/s10021-008-9166-8. URL http://link.springer.com/10.1007/s10021-008-9166-8.

Brett R. Scheffers, Lucas N. Joppa, Stuart L. Pimm, and William F. Laurance. What we know and don't know about Earth's missing biodiversity, 2012. ISSN 01695347. URL http://www.sciencedirect.com/science/article/pii/S0169534712001231.

Britta Tietjen and Andreas Huth. Modelling dynamics of managed tropical rainforests—An aggregated approach. *Ecological Modelling*, 199(4):421–432, 2006. ISSN 03043800. doi: 10.1016/j.ecolmodel.2005.11.045. URL http://www.sciencedirect.com/science/article/pii/S0304380006002869.

Cornelia M. Tobner, Alain Paquette, Dominique Gravel, Peter B. Reich, Laura J. Williams, and Christian Messier. Functional identity is the main driver of diversity effects in young tree communities, jun 2016. ISSN 14610248. URL http://doi.wiley.com/10.1111/ele.12600.

María Uriarte, Charles D. Canham, Jill Thompson, Jess K. Zimmerman, Lora Murphy, Alberto M. Sabat, Ned Fetcher, and Bruce L. Haines. Natural disturbance and human land use as determinants of tropical forest dynamics: Results from a forest simulator. *Ecological Monographs*, 79(3):423–443, aug 2009. ISSN 00129615. doi: 10.1890/08-0707.1. URL http://doi.wiley.com/10.1890/08-0707.1.

Sébastien Villéger, Norman W. H. Mason, and David Mouillot. New multidimensional functional diversity indices for a multifaceted framework in functional ecology. *Ecology*, 89(8):2290–2301,

aug 2008. ISSN 0012-9658. doi: 10.1890/07-1206.1. URL http://doi.wiley.com/10.1890/07-1206.1.

Ian J Wright, Peter B Reich, Mark Westoby, David D Ackerly, Zdravko Baruch, Frans Bongers, Jeannine Cavender-Bares, Terry Chapin, Johannes H C Cornelissen, Matthias Diemer, and Others. The worldwide leaf economics spectrum. *Nature*, 428(6985):821–827, 2004. URL http://www.nature.com/nature/journal/v428/n6985/abs/nature02403.html.

S. Joseph Wright, M. Alejandra Jaramillo, Javier Pavon, Richard Condit, Stephen P. Hubbell, and Robin B. Foster. Reproductive size thresholds in tropical trees: variation among individuals, species and forests. *Journal of Tropical Ecology*, 21(03):307–315, may 2005. ISSN 0266-4674. doi: 10.1017/S0266467405002294. URL http://www.journals.cambridge.org/abstract_S0266467405002294.

Barbara L Zimmerman and Cyril F Kormos. Prospects for Sustainable Logging in Tropical Forests. *BioScience*, 62(5):479–487, 2012. ISSN 00063568. doi: 10.1525/bio.2012.62.5.9.

List of Tables

List of Figures

Résumé : Écrire le résumé ici...

Mots clés : mots clés

Abstract: Write abstract here

Keywords: keywords